Progress in NMR Spectroscopy, 1981, Vol. 14, pp. 137–173.
© Pergamon Press Ltd. Printed in Great Britain
0079-6565/81/0401-0137 $5.00/0

MULTIPLE-QUANTUM NMR

GEOFFREY BODENHAUSEN*
Francis Bitter National Magnet Laboratory, Massachusetts Institute of Technology, Cambridge, Massachusetts, U.S.A.

(*Received* 1 *April* 1980)

CONTENTS

1. INTRODUCTION

In the broadest definition of the term, multiple-quantum NMR is concerned with the observation of nuclear transitions that are forbidden by the well-known selection rule $\Delta m = \pm 1$. The problem had been given a great deal of attention in the early days of magnetic resonance, when continuous-wave spectrometers could be used to observe forbidden transitions simply by increasing the radio-frequency power to drive the spin systems beyond the range of their linear response. In spite of some elegant examples, the potential of CW-observation of multiple-quantum transitions was never fully realized, no doubt because of difficulties with the interpretation and inconvenient instrumental requirements. The advent of Fourier transformation techniques triggered a tremendous renewal in the observation of allowed transitions, but at the same time it appeared that multiple-quantum NMR would be doomed to oblivion precisely because the basic Fourier experiment cannot be used to detect forbidden transitions. Nearly a decade went by, until the idea suddenly appeared that pulse experiments could be designed specifically to observe multiple-quantum transitions. This discovery may have been delayed because the new concept of multiple-quantum coherence could only be fruitfully explored with the development of techniques for the excitation and the detection. These ideas were perceived independently

* Present address: Physical Chemistry Laboratory, Eidgenössische Technische Hochschule, Zurich, Switzerland.

in theoretical studies of coherent optical phenomena, which inspired the pioneering NMR studies by Hashi and co-workers, and by Ernst and his group in the course of a thorough density-matrix analysis of a new class of experiments based on two-dimensional Fourier transformation. These early studies triggered an avalanche of ideas, new insights and ingenious methods, and no attempt will be made in this review to set out a chronology of the events, since some of the early papers appear to gain in clarity when treated in the light of more recent developments.

In spite of the relatively modest volume of the relevant publications, the topic presents a number of difficulties to the non-specialized reader. Most authors rely heavily on the density matrix formalism as well as on single-transition operators, thereby breaking new ground in theory as well as in methodology. Both are useful tools, but neither is necessary to gain a basic understanding of the experimental techniques.

A further difficulty arises from the wide range of the applications, which extends from isotropic solutions to single crystals, and includes oriented liquid crystalline solutions as well as polycrystalline powders, leading to a multiplicity of both quanta and jargons. Finally, the development of pulsed multiple-quantum NMR is historically intertwined with the parallel development of two-dimensional Fourier transform methods, which present their own conceptual difficulties. For these reasons, it appears that a review article could be helpful to clarify both the experimental approaches as well as the sort of physical insight one might expect from these experiments.

Much of the research has focussed on the physical properties of multiple-quantum coherence in its own right, which in many cases could not be predicted intuitively. Thus, for example, the phenomenon of the transfer of coherence between different pairs of energy levels had to be understood before applications could be envisaged. A host of techniques have been developed, such as selective detection and refocussing of inhomogeneous dephasing. These often require more than a straightforward extension of familiar single-quantum experiments, and are essential if multiple-quantum NMR is to become a practical tool. The proof of a method, however, lies in its ability to provide new insight into the physics or chemistry of a system. In this area, multiple-quantum NMR has yet to reach full maturity, although a number of promising applications have shown the new technique to provide a unique probe for molecular motion. Other applications are concerned with the simplification of spectral information, particularly for nuclei with $I \geqq 1$, where the quadrupolar splitting can be circumvented. In coupled spin systems, multiple-quantum spectra contain far less resonances than conventional spectra and the connectivity relationships of the transitions can be explored, particularly if multiple-quantum NMR is used in conjunction with double resonance. Multiple-quantum NMR can also be used for the indirect detection of nuclei with low gyromagnetic ratios coupled to nuclei with a better sensitivity such as protons. The formalism developed to describe multiple-quantum phenomena has provided new insight into the mechanism of spin decoupling, leading to new applications where decoupling had not been used before as a means of simplifying spectral information. Finally, a number of traditional experiments which appear in no way related to multiple-quantum effects, such as the ubiquitous inversion-recovery sequence, turn out to be susceptible to serious systematic errors arising from multiple-quantum interference.

This review has been subdivided such as to enable a hasty reader to move directly from the discussion of the basic pulse experiment (Section 3) to the applications in Sections 6 and 8, leaving the refinements in Sections 2, 4, 5 and 7 to a more specialized audience.

2. SLOW-PASSAGE OBSERVATION

A decade or so before the advent of pulsed Fourier transform methods. Anderson[1] and Kaplan and Meiboom[2] demonstrated that double-quantum transitions can be observed with a continuous-wave NMR spectrometer. The mechanism involved in this experiment is fundamentally different from the pulsed multiple-quantum techniques, yet the basic information content of the two experiments is very similar, and a brief survey of the continuous-wave literature should reveal both the analogies and the decisive advantages of the pulsed techniques. The CW experiments employ a strong monochromatic RF field to perturb the spin system, in such a manner that the eigenstates in the presence of the RF field are made up of linear combinations of the eigenfunctions of the free Hamiltonian. The formalism involves the diagonalization of the Hamiltonian in a rotating frame where the RF field appears static, much like the treatment of double resonance experiments. The mixed states are no longer subject to the rigorous selection rule $\Delta m = \pm 1$, since the matrix elements of the I_x operator no longer vanish for transitions which, by analogy to the unperturbed system, can be loosely labelled with $\Delta m = \pm 2$, ± 3, etc. These transitions thus become amenable to observation by ordinary CW NMR. By a fortunate coincidence, they are much less prone to saturation than their single-quantum counterparts, and can be observed with the *same* strong RF field which is also responsible for the mixing of the states. Thus CW multiple-quantum NMR is in effect a double-resonance experiment where the RF fields used for the perturbation and the observation are one and the same.

In conventional NMR, the resonance frequency ω_{rs} of a $\Delta m = \pm 1$ transition is simply determined by the difference of eigenstate energies $(E_s - E_r)/\hbar$. If this rule

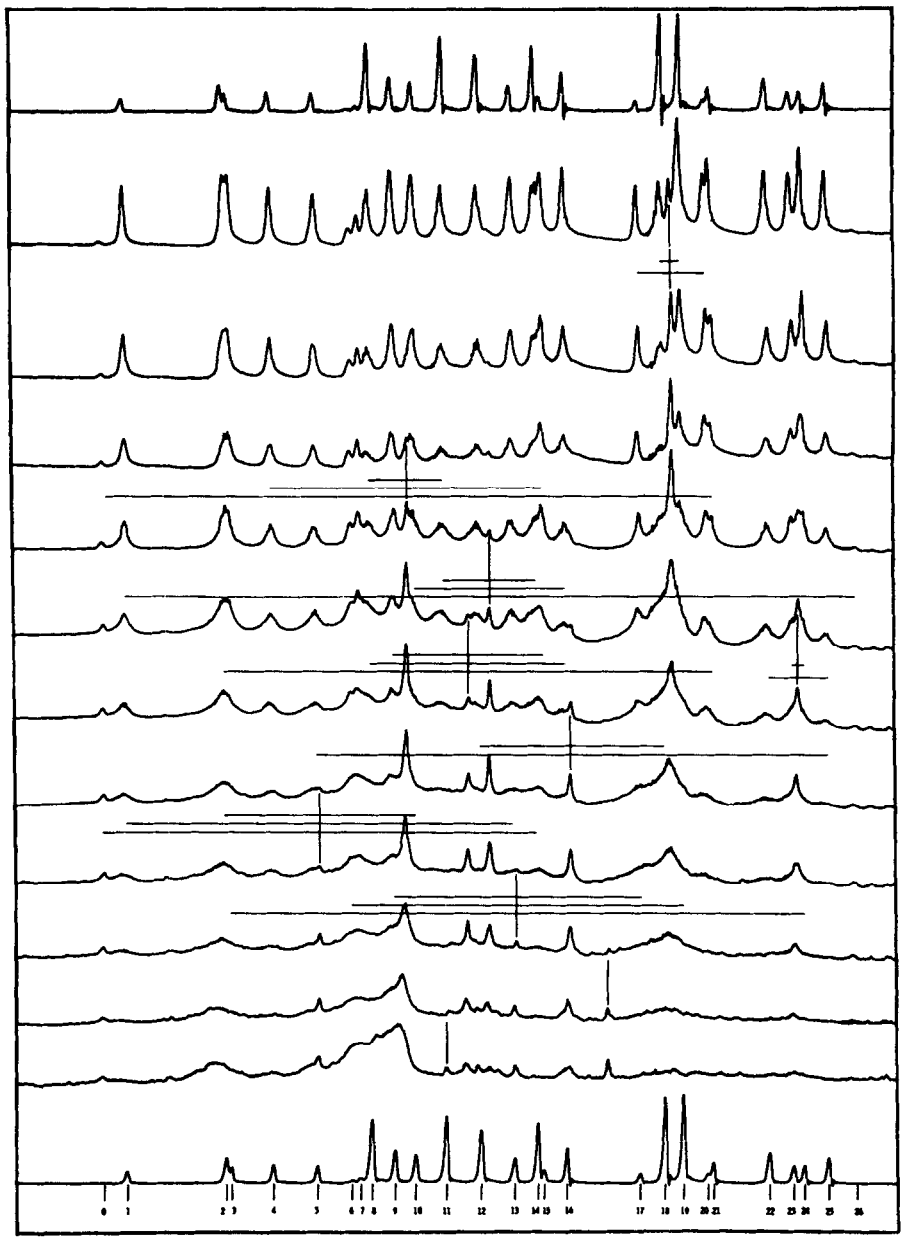

FIG. 1. High-resolution slow-passage proton spectra of trivinylphosphine, recorded with increasing RF power levels (except for the unsaturated spectra at top and bottom.) The double and triple quantum transitions are indicated by vertical lines, with crossbars to identify pairs of connnected single-quantum transitions. In the slow-passage method, the various multiple-quantum signals appear at different RF levels, and the signals can only be distinguished from the background because of their linewidth and RF field dependence. (Anderson, Freeman and Reilly.[4])

were extended to double-quantum transitions, one would expect to observe NMR phenomena at twice the Larmor frequency. It turns out that such an experiment is not possible; instead, a p-quantum transition between the levels r and s appears at $\omega_{rs}^{p} = (E_s - E_r)/(p\hbar)$. This relationship can be readily grasped by assuming that the spin system actually absorbs p quanta from the RF field, although this concept should be applied with caution and rarely provides insight into the discussion of pulsed techniques. The theoretical foundations of CW multiple-quantum NMR were discussed by Yatsiv[3] in terms of perturbation theory, while Anderson, Freeman and Reilly[4] simplified the interpretation and provided an elegant demonstration. The latter authors used multiple-quantum spectra as an aid in the assignment of the proton spectrum of trivinyl-phosphine, which at 60 MHz consists of some thirty lines belonging to two superimposed ABC patterns (Fig. 1, top spectrum.)

It is well known that the energy levels of each ABC system can be represented graphically by a cube,[4] but the assignment of the individual spectral resonances to the edges of the cube is no trivial enterprise. Consider for example a set of four allowed transitions which together span one of the faces of the energy-level cube. A double-quantum transition[1,4] connects the top and bottom states ψ_1 and ψ_4, while the progressive pairs of single-quantum transitions $\omega_{12}+\omega_{24}$ and $\omega_{13}+\omega_{34}$ connect the same top and bottom levels through the intermediate states ψ_2 and ψ_3. It follows that the double-quantum frequency must obey the relationship

$$\omega_{14} = (\omega_{12}+\omega_{24})/2 = (\omega_{13}+\omega_{34})/2.$$

Hence the four single-quantum resonances associated with one of the faces of the cube must be symmetrically disposed on either side of the double-quantum signal, and they can be readily identified because of this symmetry requirement. The spectra shown in Fig. 1 illustrate both the potential and some of the problems associated with this technique. The double and triple-quantum transition frequencies, indicated by vertical bars in Fig. 1, can be distinguished by their narrow linewidths, which suffer less from saturation than the background of broadened single-quantum absorption. The RF power must be incremented in small steps, since no single power level is adequate for the observation of all multiple-quantum transitions. The amplitude of the double-quantum signals rises quickly with the third power of the RF field strength, and drops equally quickly when saturation sets in.[3,4] The horizontal bars in Fig. 1 extend sideways from the double-quantum signals to point at the symmetrical pairs of single-quantum transitions. The information contained in Fig. 1 allows an immediate assignment of the single-quantum spectrum to the energy level diagram, since the transitions which share a common energy level are readily identified, much like in spin-tickling experiments.

It is not surprising perhaps that the experimental difficulties associated with CW multiple-quantum NMR have discouraged widespread applications, with a few notable exceptions, such as the work of McLauchlan, Whiffen and Cohen[5,6,7] who used double-quantum NMR to determine the relative signs of J-couplings, as well as the studies of Musher[8] and Martin *et al.*[9] who focussed their attention on geminal proton–proton couplings.

Apart from the need to guess the appropriate RF power level, the principal drawback of the CW method appears to be the presence of a background of broad lines due to saturated single-quantum absorption. This lack of selectivity presents particular problems when the experiment is designed to determine relaxation parameters. Worvill[10] has shown the subtle effects of different relaxation mechanisms on the CW multiple-quantum spectra of strongly coupled ABC systems. Apart from the distortions due to the background, the analytical expressions for the lineshapes of the multiple-quantum resonances in terms of the Redfield relaxation theory, which have been discussed by Hoffman[11] and by Gestblom *et al.*,[12,13] tend to be rather involved. This is in sharp contrast to pulsed multiple-quantum NMR, which provides a straightforward measure of transverse relaxation that can often be related directly to the spectral densities of motion without requiring a cumbersome lineshape analysis.

Further complications arise in CW experiments from the fact that a strong, continuous RF field can cause a multiple-quantum resonance to shift in frequency[3,4] in analogy to Bloch–Siegert effects.[14] Bucci *et al.*[15] have confirmed these effects quantitatively and formulated a new theoretical approach which circumvents the rotating frame by using the second quantization formalism.[16] This work led to multiple-quantum experiments with two different RF fields which involve the absorption of p photons from one wave and the simultaneous emission of $p \pm 1$ photons to the other wave.[17] Such processes are quite distinct from those involved in pulsed techniques, which are based on the concept of coherence rather than on the accounting of photon processes.

Double-quantum effects can be observed in CW NMR in partially oriented deuterated systems, such as in nematic liquid crystals for example, where the anisotropy of the medium lifts the degeneracy of the $(-1,0)$ and the $(0,+1)$ transitions of $I = 1$ spin systems. The splitting of the resulting doublets is proportional to the order parameter S and to the quadrupolar interaction in the corresponding rigid lattice. When the RF power is increased, a third resonance appears in the middle, which arises from the $(-1,+1)$ double-quantum transition. Such effects have been observed by Biemond, Lohman and MacLean[18] in perdeuterated benzene in an environment where the anisotropy was generated by applying a strong electric field to cause a partial alignment of polar solvent molecules. In the lyotropic liquid crystals studied by Wennerström, Persson and Lindman,[19] the samples are not oriented by the magnetic field and there is a distribution of orientations which tends to spread the allowed deuterium transition frequencies over a wide spectral range, not unlike a rigid powder pattern. For all orientations however, the central double quantum transition appears at the same resonance frequency, leading to a sharp feature in the CW spectra which stands out in contrast to the broader allowed transitions. A related effect has been observed in ^{23}Na NMR in lyotropic liquid crystals,[20] where the triple-quantum transition of the $I = 3/2$ nucleus has a frequency which is independent of the orientation. The two double-quantum transitions in ^{23}Na however are subject to powder broadening. Double-quantum transitions have also been reported in polycrystalline powders by Creel, von Meerwall and Barnes,[21] who

considered ^{14}N, a nucleus of particular interest because the quadrupolar interaction can be of the same order of magnitude as the Larmor frequency.

A number of well-known NMR experiments combine CW excitation with the principle of indirect detection. Although this type of experiment has in some cases been superseded by a more powerful Fourier transform counterpart, some instances remain where CW excitation cannot be avoided and multiple-quantum phenomena are likely to occur, because the strength of the RF field is often sufficient to drive the spin systems beyond the range of linear response. Such a situation arises for example in depolarization experiments used to obtain NMR spectra of short-lived radioactive nuclei, where it is necessary to enhance the population differences much beyond the Zeeman polarization achieved in a static magnetic field. Nuclear reactions such as $^{11}B(d,p)^{12}B$ can be used for this purpose,[22] or else it is possible to irradiate a sample of ^{7}Li with polarized neutrons to generate ^{8}Li.[23] In both cases, the population differences between the states can be measured indirectly by observing the β-radiation emitted by the decaying nuclei (the half-life times are 20.4 ms and 0.84 s respectively). The polarizations typically approach a few percent, and greatly exceed the 10^{-5} or so typical for high-field NMR in a static field. The actual NMR spectrum is obtained by sweeping a strong CW RF field which tends to equalize the populations, leading to a sharp drop in the polarization of the emitted β-particles. In order to achieve a dramatic effect, strong RF fields must be applied, thus setting conditions appropriate for multiple-quantum phenomena.

The NMR spectrum of oriented ^{12}B ($I = 1$) studied by McDonald and McNab[22] consists of a doublet due to the allowed transitions with a single sharp resonance in the center arising from the $(-1, +1)$ double-quantum transition. This could be established unequivocally by adiabatic fast passage applied to the central transition alone, which causes the populations of the $m = -1$ and $m = +1$ levels to interchange selectively. The NMR spectrum of ^{8}Li ($I = 2$) obtained by Dubbers *et al.*[23] features all possible transitions: four single, three double, two triple and one quadruple-quantum transition. The transitions of higher order are more effective in the depolarization process and tend to dominate the spectra, as can be seen in Fig. 2.

These observations may appear to be rather esoteric and limited in scope, but they carry a message that should be relevant for more mundane NMR experiments involving indirect detection, such as INDOR for example,[24] where the S spin resonance is detected through the NMR response of a coupled spin I. In this type of experiment, the RF field strength B_1^S is sufficient to induce tickling effects[25] and should be expected to cause multiple-quantum phenomena, both in oriented samples when the S spectrum is subject to quadrupolar splittings, as well as in isotropic media with homonuclear interactions among different S nuclei.

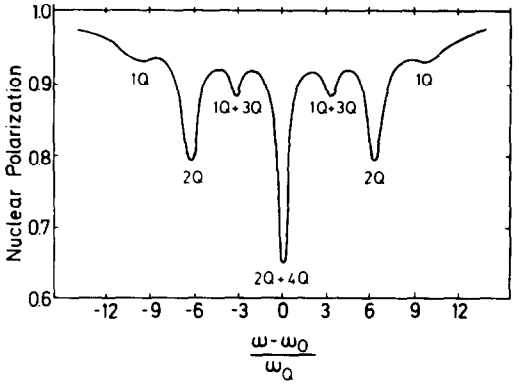

FIG. 2. Theoretical slow-passage NMR spectrum of the short-lived ^{8}Li nucleus ($I = 2$) in an oriented single crystal of $LiTaO_3$. The strength of the RF field (equal to one-sixth of the separation of two allowed transitions) is sufficient to induce up to four-quantum transitions. The sample is prepared by irradiation with polarized neutrons, and the NMR transitions are recorded by monitoring the drop in the population differences upon RF irradiation, hence the negative sign of the signals. (Dubbers *et al.*[23])

In electron paramagnetic resonance, continuous-wave techniques still enjoy widespread popularity in spite of the advent of Fourier transform technology. Rawson and Beringer[26] observed mysterious additional lines in the EPR spectrum of atomic oxygen, which were later shown to arise from double-quantum absorption by Hughes and Geiger[27] and by McDonald.[28] Double and triple-quantum transitions were also observed in Mn^{2+} in a magnesium oxide host lattice by Sorokin, Gelles and Smith.[29] The five electron spin transitions $(-5/2, -3/2), (-3/2, -1/2) \ldots (+3/2, +5/2)$ are split because of the coupling to the lattice field. When the RF power is increased, additional lines appear which correspond to the electron spin double-quantum transitions $(-3/2, +1/2)$ and $(-1/2, +3/2)$. These experiments were extended by Chiarini, Martinelli and Ranieri[30] to cases with accidentally overlapping single- and double-quantum resonances.

Dalal and Manoogian[31] recently observed double-quantum transitions in electron–nuclear double resonance (ENDOR) in Cr^{3+}, which have the gratifying property of providing greatly enhanced resolution compared to single-quantum lines.

Closely related phenomena were observed by Oka and Shimizu[32] in microwave spectroscopy, where the rotational double and triple-quantum transitions ($J = 0, 2$) and $(0, 3)$ of CD_3CN could be observed, which behave in a manner similar to NMR phenomena.[33]

Much of the emphasis of the slow-passage NMR work appears to be on the dangers of erroneous interpretations that arise if multiple-quantum phenomena are not properly recognized. In liquid

crystalline systems for example, central peaks in deuterium spectra have been explained by invoking mixtures of isotropic and anisotropic phases,[19] while the central spike in the solid-state spectra of ^{12}B has been attributed to a hypothetical cubic environment in the lattice.[34] To avoid such pitfalls, it is advisable to verify the RF power dependence of the CW spectra or, if possible, to avoid multiple-quantum phenomena altogether by using Fourier transform NMR.

It should be stressed that the CW approach is not suitable for the observation of zero-quantum transitions ($\Delta m = 0$), which have a number of interesting properties that can only be made accessible in pulsed experiments.

3. THE BASIC PULSE EXPERIMENT

The familiar pulse experiment which is universally employed in conventional NMR for the observation of allowed transitions is built on the idea that excitation and observation can be separated into subsequent time intervals. A radio-frequency pulse prepares the spin system to bring eigenstates separated by $\Delta m = \pm 1$ into coherent superposition, that is to say, the inherent time-dependence of each state, normally random in thermal equilibrium, acquires a phase coherence across the ensemble. This coherence, which is better known as transverse magnetization, induces a free induction decay signal in a receiver coil because it is capable of emitting dipolar radiation. The rigorous definition of the coherence is based on the expansion of the time-dependent wave-function of the system in terms of stationary basis functions, usually eigenfunctions of the free Hamiltonian:

$$\Psi(t) = \sum_{i=1}^{N} c_i(t)\psi_i \tag{1}$$

A coherence between states ψ_r and ψ_s exists when the ensemble average of the product of coefficients

$$\sigma_{rs}(t) = \overline{c_r(t)c_s^*(t)} \tag{2}$$

does not vanish.[35] The elements $\sigma_{rs}(t)$ defined by this equation are tabulated in the form of a Hermitian $N \times N$ matrix which is known as the density matrix. In the case where

$$\Delta m_{rs} = m_r - m_s = \pm 1$$

in weakly coupled spin 1/2 systems, a density matrix element is essentially the same as a classical transverse magnetization vector M_{rs}:[36]

$$M_{xrs}(t) = \mathrm{Re}\,\{\sigma_{rs}(t)\} \tag{3}$$

$$M_{yrs}(t) = -\mathrm{Im}\,\{\sigma_{rs}(t)\} \tag{4}$$

where the negative sign compensates for a trivial contradiction in the conventional sense of rotation. In the following pages, extensive use will be made of the σ_{rs} notation, which is a convenient symbol for the amplitude and phase of a coherence and does not necessarily demand any further understanding of the density matrix formalism.

In a general case, most σ_{rs} terms do not contribute directly to the signal S, and those that are capable of inducing a signal are weighted by the matrix element of the I_y operator, which corresponds to the square root of the transition probability as it is known in slow-passage NMR and vanishes for all transitions that do not fulfill the $\Delta m = \pm 1$ requirement. The free induction signal observed in a Fourier experiment is described by:[35,37]

$$S_y(t) = \mathrm{tr}\,\{\sigma I_y\} = \sum_r \sum_s \sigma_{rs} I_{ysr} \tag{5}$$

where the phase sensitive detector is assumed to be set up such as to "see" the y-component of the magnetization in the rotating frame. This equation in effect projects those parts of the density matrix σ that are capable of coupling to the receiver.

3.1. *Invisible Coherence*

Clearly, the coherence σ_{rs} defined in equation (2) need not be restricted to pairs of states ψ_r and ψ_s separated by $\Delta m_{rs} = \pm 1$. In fact, any arbitrary coherence σ_{rs} can be made non-zero by preparing the spin system with appropriate RF pulses. At first, this appears to be a trivial generalization of the idea of transverse magnetization. To paraphrase Saint-Exupéry however, *l'essentiel n'est pas visible.*[38] More prosaically, an arbitrary coherence σ_{rs} with $\Delta m \neq \pm 1$ is not capable of inducing a signal in the receiver, and a trick is required if σ_{rs} is to be made observable: a pulse must be applied to transfer the invisible coherence σ_{rs} into observable magnetization σ_{pq} which must satisfy the condition $m_p - m_q = \pm 1$. This concept of coherence transfer, which is not commonly encountered in conventional Fourier transform experiments, is embodied in a basic pulse experiment depicted schematically in Fig. 3, which has emerged

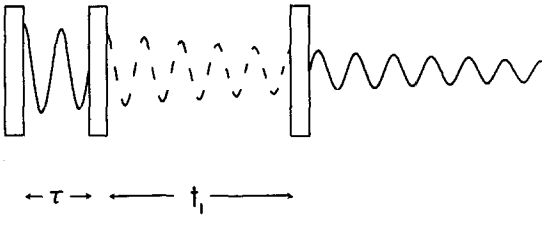

FIG. 3. Simple pulse sequence for the observation of multiple-quantum coherence in systems which can be subjected to non-selective pulses. The first 90° pulse generates ordinary single-quantum magnetization, which precesses in the transverse plane of the rotating frame for a time τ. A second 90° pulse converts the magnetization into invisible multiple-quantum coherence, which can be recalled after an evolution period t_1 by a 90° monitoring pulse. The receiver is activated after the third pulse only, and the experiment must be repeated for a number of t_1-values to map out the time evolution of the invisible coherence.

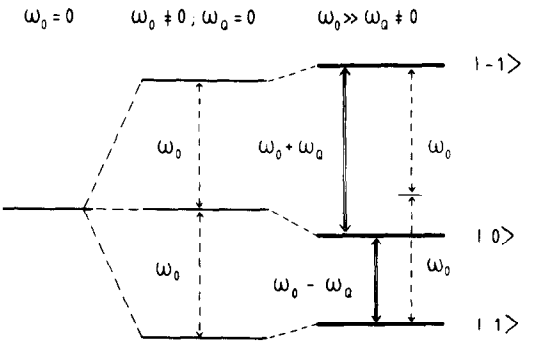

FIG. 4. Energy-level diagram for a single oriented spin $I = 1$. The quadrupole interaction lifts the degeneracy of the $(-1, 0)$ and $(0, +1)$ transitions, which appear at $\omega_0 \pm \omega_Q$ in the single-quantum spectrum. The double-quantum transition $(-1, +1)$, however, is invariant to the quadrupole interaction, provided the latter is small compared to the Larmor frequency.

as one of the most successful tools in multiple-quantum NMR.

Consider the simplest case where double-quantum coherence can occur, a single spin $I = 1$ oriented with respect to the static field. Such a system can be found in a single crystal of some partially deuterated material, or else in a deuterated solute in a nematic liquid crystalline solvent for example. The two single-quantum transitions ω_{12} and ω_{23} of the three level spin system shown in Fig. 4 are separated by $2\omega_Q$, which may vary typically between a few hertz and some 100 kHz for deuterons, depending on the extent of motional averaging.

The pulse sequence in Fig. 3 initially excites the transverse magnetization by a strong 90° pulse ($\gamma B_1 \gg 2\omega_Q$), which may be described formally by a unitary transformation of the density matrix by exponential operators[35,37,39]

$$\sigma^+ = \exp\{-i\alpha I_x\}\sigma^- \exp\{+i\alpha I_x\} \tag{6}$$

where the symbols σ^- and σ^+ refer to the density matrix just before and just after a pulse of duration τ_p with a flip angle $\alpha = \gamma B_1 \tau_p$, applied along the x-axis of the rotating frame. If the system is in thermal equilibrium just before the excitation, equation (6) simplifies to

$$\sigma^+ = I_z \cos\alpha - I_y \sin\alpha \tag{7}$$

which amounts to a simple rotation of the magnetization about the x-axis of the rotating frame. Thus, for $\alpha = 90°$, the only non-vanishing elements of the σ^+ matrix are single-quantum coherences, since the elements I_{yrs} are zero except for $\Delta m = \pm 1$. This is a general rule if a system in thermal equilibrium is excited by a single, "hard" pulse. The subsequent evolution of the transverse magnetization is described by another unitary transformation

$$\sigma(\tau) = \exp\{-i\mathcal{H}\tau\}\sigma^+ \exp\{+i\mathcal{H}\tau\} \tag{8}$$

which boils down to a simple phase precession, provided the basis functions ψ_i are eigenfunctions of the free Hamiltonian:

$$\sigma_{12}(\tau) = \sigma_{12}^+ \exp\{-i\omega_{12}\tau\} \tag{9}$$

$$\sigma_{23}(\tau) = \sigma_{23}^+ \exp\{-i\omega_{23}\tau\} \tag{10}$$

all other elements of the σ matrix being either complex conjugates or zero. The second 90° pulse in Fig. 3, which may also be described by equation (6), has a dramatic effect. If the magnetization vectors σ_{12} and σ_{23} are allowed to precess until the end of the τ-interval such as to both appear along the x-axis of the

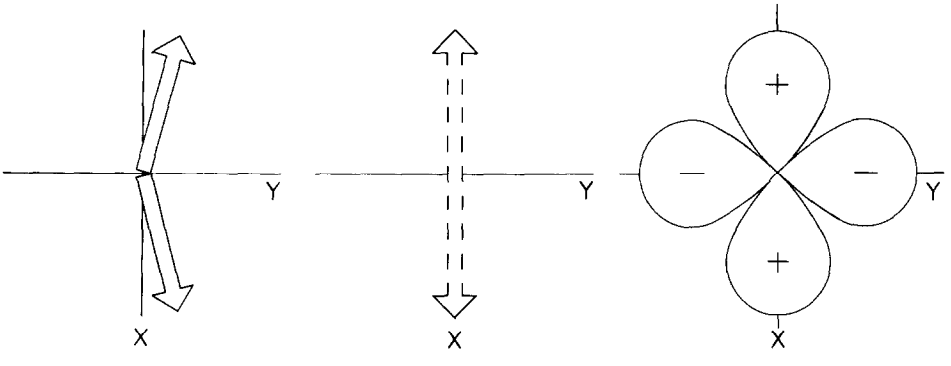

FIG. 5. (*a*) The two single-quantum magnetization vectors of a single oriented deuteron are initially flipped along the y axis of the rotating frame and precess until they are aligned with the $+x$ and $-x$ axes. (*b*) The second 90° pulse transforms the observable magnetization into invisible double-quantum coherence, depicted by a dotted double-pointed arrow (Hoatson and Packer[41]). The phase and precession properties of the double-quantum coherence are represented adequately by this "ghost" which precesses in the usual rotating frame at a frequency determined only by the chemical shift $\Delta\omega$. Because of its symmetry, the coherence is invariant under a 180° phase-shift. (*c*) A more sophisticated graphical representation of the double-quantum coherence uses a d-orbital function (Pines *et al.*[46]). The positive lobes correspond to the tips of the double-pointed arrow. Because of the negative lobes the sign of the magnetization observed after the monitoring pulse is reversed when the coherence is rotated through 90°. The d-orbital is invariant under a 180° pulse applied either along the x or y axis, but changes sign when the 180° pulse is shifted in phase through 45° (see Section 7).

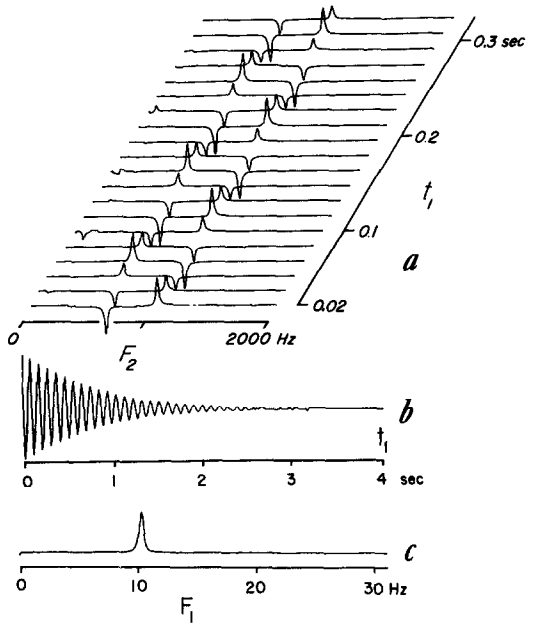

FIG. 6. Double-quantum experiment for a single oriented deuteron. The algebraic amplitudes of the two antiphase signals depend on the phase of the double-quantum coherence just before the monitoring pulse. The time evolution of the invisible coherence is mapped out in the "interferogram" (b), obtained by recording the peak heights in (a) as a function of t_1. This signal may be subjected to a second Fourier transformation which leads to the double-quantum frequency domain F_1. In this experiment, the double-quantum phase is determined not by free precession but by a combination of refocussing and phase-shifting. Reproduced from reference 40.

rotating frame, but with opposite phases, the single-quantum coherences vanish as if by magic and a double-quantum coherence σ_{13} suddenly appears instead.[40,41] If the receiver were activated at this time, no signal would be observed, because the antiphase magnetization components are killed by the pulse, a process which seems to defy the intuition. Note that the Bloch picture applicable to isolated spin 1/2 nuclei would be misleading in this case, since an RF field which is collinear with the magnetization vectors would not be expected to have any effect at all. The metamorphosis of the coherence of a spin $I = 1$ has been described pictorially by Hoatson and Packer.[41] As a result of the second 90° pulse, the single-quantum vectors in Fig. 5 suddenly vanish, only to be replaced by a double-pointed arrow that may be seen as the "ghost" of the deceased vectors. A more general treatment[40,41] shows the amplitude of the double-quantum coherence to depend on the phases of the single-quantum magnetization vectors just before the second pulse. These phases are determined by ω_{12} and ω_{23}, which in turn depend on the offset $\Delta\omega$ and the quadrupolar splitting ω_Q:

$$|\sigma_{13}| = |\cos \Delta\omega\tau \sin \omega_Q\tau|. \qquad (11)$$

To convert the double-quantum coherence back into observable magnetization, the single-quantum elements σ_{12} and σ_{23} have to be resurrected by a third 90° pulse (the so-called "monitoring pulse") which generates two new magnetization vectors that are again collinear with the RF field in the rotating frame, and appear automatically with opposite phases. By stepping the interval t_1 which separates the excitation and the monitoring pulse in Fig. 3, one can follow the time evolution of the double-quantum coherence σ_{13}. The experiment must be carried out in a point-by-point manner, since the monitoring pulse interrupts the precession of the double quantum coherence. This step-by-step approach may appear cumbersome, but has in fact become routine in a growing class of experiments known under the general heading of two-dimensional spectroscopy, which need not necessarily be much more time-consuming than one-dimensional techniques.

A typical double-quantum experiment is shown in Fig. 6. The deuterium spectrum of deuterochloroform in polybenzylglutamate features a quadrupolar splitting because of the alignment of the polymer in the static external field B_0. The spectra obtained with the pulse sequence in Fig. 3 for increasing values of t_1 all show lines at ω_{12} and ω_{23} in opposite phase. The t_1-oscillation reflects the phase precession of the double-quantum coherence and can be mapped out by compiling the peak heights as a function of t_1 to obtain an "interferogram" (Fig. 6b), which may be subjected to a second Fourier transformation to identify the frequency and the time constant of the decay of the double-quantum coherence.

3.2. *Precession and Phase*

A number of peculiar properties of the double-quantum coherence, which are formally described by the density-matrix, may benefit from a phenomenological discussion because they do not seem to fit the intuition of a single-quantum NMR spectroscopist. At the time of writing, there is no general agreement on a graphical representation analogous to magnetization vectors, which have proven so useful in discussing a wide variety of NMR phenomena. The free precession frequency of the σ_{13} coherence of a single deuteron, described by equation (8), turns out to be equal to *twice* the offset $\Delta\omega$ of the chemical shift with respect to the RF carrier:

$$\sigma_{13}(t) = \sigma_{13}(o) \exp\{-i2\Delta\omega t\}. \qquad (12)$$

In general, a p-quantum coherence appears to see a p-fold offset. Thus if the transmitter frequency is changed, all p-quantum signals experience a p-fold frequency jump. Obviously, the double-quantum signals do not appear in the centre of connected single-quantum transitions as is the case in CW NMR. This behaviour can be rationalized in either of two ways. In analogy to magnetization vector pictures, the σ_{13} coherence can be described in a special rotating frame (the "double-quantum

frame"[41,42]) as a vector precessing at $2\Delta\omega$, the factor 2 being simply borrowed from equation (12). Alternatively, the double-quantum coherence can be visualized as the "ghost" or double-pointed arrow depicted in Fig. 5, which precesses at $\Delta\omega$ like an ordinary magnetization vector in the conventional rotating frame. Since a rotation through 360° brings the "ghost" twice to its position of departure, the coherence *appears* to rotate at twice the offset frequency $\Delta\omega$. This picture is also consistent with the characteristic response of multiple-quantum coherence to phase-shifts of the RF field. If the excitation pulses are shifted in phase through an angle ϕ, the double-quantum term "sees" twice this shift:

$$\sigma_{13}(\phi) = \sigma_{13}(o)\exp\{-i2\phi\}. \tag{13}$$

The coherence is thus invariant under a 180° phase shift of the excitation sequence. In general, a p-quantum coherence experiences a p-fold phase shift. This property has been explored by Hatanaka, Ozawa and Hashi,[43] by Vega and Pines[44] and by Wokaun and Ernst[45] who used phase shifts to characterize the order p of multiple-quantum coherence.

It is apparent in Fig. 6 that the signals observed after the monitoring pulse appear upside down if the double-quantum coherence precesses through one-half of its period. To explain this in phenomenological terms, the double-pointed arrow has to be refined. A more satisfying representation is a function reminiscent of an atomic d-orbital.[46] If the azimuthal angle in the xy plane of the rotating frame is defined by $\theta = \text{arctg}\,(x/y)$, the real d-orbitals at the intersection of the transverse plane have the form

$$d_{x^2-y^2} = \cos 2\theta \tag{14}$$

$$d_{xy} = \sin 2\theta. \tag{15}$$

The first function has positive lobes along the x-axis (corresponding to the arrows of the Hoatson-Packer "ghost" in Fig. 5) and negative lobes along the y-axis of the rotating frame. The second function is orthogonal in terms of the overlap integral and appears rotated through 45° with respect to the first function. The precession of the coherence is represented by introducing a time-dependent argument $\mathrm{d}(t) = \cos 2(\theta + \Delta\omega t)$. The algebraic amplitude of the observable magnetization created by the monitoring pulse is described phenomenologically by the overlap integral of the precessing double-quantum function with a stationary function whose phase is tied to the phase ϕ' of the monitoring pulse:

$$\sigma_{12} = -\sigma_{23} = \int_0^{2\pi} [\cos 2(\theta+\phi+\Delta\omega t)] \times [\cos 2(\theta+\phi')]\,\mathrm{d}\theta \tag{16}$$

where the RF phase ϕ of the initial excitation has been included in the argument. After a 45° precession, the signal vanishes since the functions are orthogonal, while the integral changes sign after a 90° rotation of the coherence. The quadrupolar symmetry of the d-orbital function provides an intuitive grasp of the failure of the double-quantum coherence to emit dipolar radiation and to couple to the receiver coil, and the model provides an attractive explanation for the echo phenomena discussed in Section 7. The extension to triple-quantum coherence requires a function of the type $f = \cos 3(\theta+\phi+\Delta\omega t)$ which has a symmetry similar to an f-orbital function with three positive lobes bisected by three negative lobes. A phase-shift of 30° causes the overlap integral to vanish, while a 120° rotation is equivalent to the identity operation, thus causing an apparent rotation that is three times as fast as the actual precession of the function.

4. ALTERNATIVE EXCITATION METHODS

The double-pulse excitation discussed in the previous section, which was introduced by Aue, Bartholdi and Ernst,[47] is based on strong, non-selective 90° pulses which must cover all allowed transitions uniformly. The idea turns out to be applicable to a wide variety of systems, such as scalar coupled nuclei in isotropic solutions[47] and spin systems with dipolar[48] and quadrupolar[40,41] interactions in oriented liquid crystals. In some systems, however, the double pulse excitation technique needs to be refined, and alternative methods may be required when the strength of the transmitter pulses is insufficient to ensure a uniform excitation of the single-quantum spectrum.

4.1. *Offset-Independent Excitation*

One of the inconvenient features of the 90°–τ–90° sequence is the dependence of the multiple-quantum excitation on the offset $\Delta\omega$ of the transmitter as expressed in equation (11). This problem can be readily eliminated by inserting a 180° refocussing pulse in the middle of the τ-interval. Just before the second 90° pulse transfers the magnetization into multiple-quantum coherence, the precession due to the chemical shift and the inhomogeneity of the static field is cancelled, while the 180° pulse does not affect the phase precession associated with quadrupolar or homonuclear scalar and dipolar interactions. The 90°–$\tau/2$–180°–$\tau/2$–90° sequence has been used by Müller[49] in heteronuclear scalar coupled systems and has been the subject of a detailed calculation for oriented $I = 1$ spins.[41] The Berkeley group,[50] however, has demonstrated a variety of applications to dipolar coupled spins with $I = 1/2$.[50] Unlike other excitation techniques, the modified double-pulse approach does not require a detailed knowledge of the resonance frequencies and circumvents the need for a careful adjustment of the transmitter frequency. The sequence has the additional virtue of

differentiating between multiple-quantum coherence of even and odd orders, as discussed in Section 4.9.

4.2. *Broadband Excitation*

It is obvious that the choice of the τ-interval in the $90°$–τ–$90°$ sequence is critical to achieve efficient multiple-quantum excitation, as can be seen in the case of a single oriented deuteron, where the τ-interval and the offset must be adjusted simultaneously to suit the demands of the coherence transfer.[40] In more complex systems however, no single τ-value can be found to optimize the excitation of all multiple-quantum coherences. Although the pulses are assumed to be strong, and thus capable of broadband excitation in the single-quantum domain, it is no trivial matter to achieve a uniform excitation in the multiple-quantum domain. Analytical calculations of the excitation tend to be unwieldy for all but the simplest systems, and in many cases τ is best determined by trial and error. Drobny *et al.*[48] have proposed a broadband excitation technique where the interval of the $90°$–τ–$90°$ sequence is either varied in a pseudo-random manner or simply incremented in regular steps. For each τ-value, a complete set of experiments must be carried out for all t_1-values, and it may be necessary to calculate an absolute-value mode of the multiple-quantum spectrum before averaging over the various τ-values to avoid the cancellation of signals with opposite phases. In practice, Drobny *et al.*[48] used a dozen τ-values, regularly spaced between 9.6 and 10.7 ms, to achieve an essentially uniform excitation of the multiple-quantum coherences in the dipolar-coupled proton system of benzene oriented in a nematic liquid crystal.

A more rigorous approach has been developed in view of the uniform excitation of double-quantum coherence in a polycrystalline powder of deuterated material.[50] The quadrupolar powder pattern observed in single-quantum NMR, which typically spans a width in excess of 100 kHz, can be thought of as a superposition of quadrupolar doublets, each of which behaves exactly like an oriented single deuteron, except that the splitting $2\omega_Q$ depends on the orientation of the crystallites with respect to the static magnetic field. According to equation (11), the efficiency of the $90°$–τ–$90°$ excitation depends on

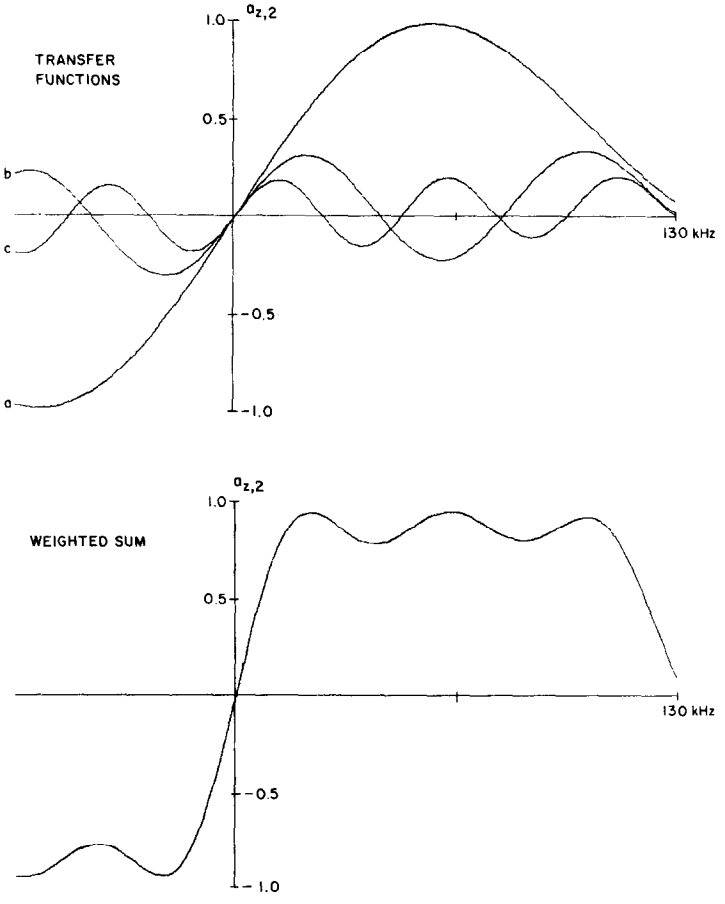

FIG. 7. The $90°$–τ–$90°$ excitation technique can be made efficient over a wide range of quadrupolar, dipolar or scalar splittings by using three different τ-intervals. The weighted sum amounts to a uniform excitation. Maximum quadrupolar splitting 260 kHz, RF field strength 100 kHz, τ = 2.25 μsec, 10 μsec and 17.75 μsec. (Wemmer[50].)

$\sin \omega_Q \tau$ and $\cos \Delta\omega\tau$. In this case the offset dependence is avoided simply by positioning the transmitter in the centre of the powder pattern. The key to the excitation problem is the use of three different τ-values which relate as odd harmonics (for example $\tau = 3$, 9 and 15 μs) to provide the most efficient excitation for different parts of the powder ($\omega_Q/(2\pi) = 83$, 88 and 17 kHz respectively).

The excitation functions shown in Fig. 7 have been refined to account for the effects of finite pulse power, and indicate that a weighted linear combination of the three experiments (each of which may be seen as a component of a Fourier series) amounts to a reasonably uniform double-quantum excitation. As in all excitation methods, the efficiency drops sharply for $\omega_Q \cong 0$, when the allowed transitions are nearly degenerate and the excitation of multiple-quantum coherence becomes impossible.

4.3. *Selective Single-Quantum Pulses*

Many spin systems cannot be excited by non-selective pulses because the magnitude of the splittings demands prohibitive power levels of the RF transmitter. The work of Hashi and co-workers[51] on ^{27}Al presents an excellent example. The experiments were carried out with single crystals of Al_2O_3 oriented in such a way as to align the electric field gradient with the static field. The $I = 5/2$ ^{27}Al nucleus has five allowed transitions which appear at intervals of some 360 kHz in the single-quantum NMR spectrum, the Larmor frequency being *ca.* 10 MHz in a field of 0.9 T. All experiments reported so far are concerned with only three of the six energy levels, in effect reducing the problem to a "pseudo spin $I = 1$". This presents obvious similarities with ^{14}N which is an important nucleus for structural studies of peptides,[52,53] where the quadrupolar splitting tends to be even greater than in ^{27}Al. The energy levels involved in Hashi's experiments correspond to $m = -3/2$, $-1/2$ and $+1/2$, and will be referred to as levels a, b and c respectively.

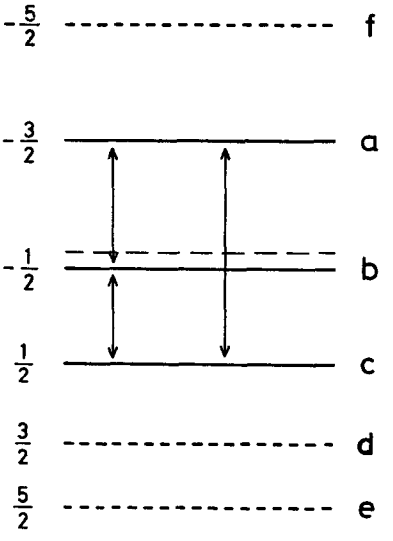

FIG. 8. Energy level diagram appropriate for ^{27}Al ($I = 5/2$) in an oriented single crystal of Al_2O_3. Only three energy levels are involved in the experiments of Hashi and co-workers.[43,51] The separation between the allowed transitions (a, b) and (b, c) is about 360 kHz.

A 90° pulse is first applied to the (a, b) transition to generate single-quantum coherence σ_{ab}. The transfer into double-quantum coherence σ_{ac} can be achieved by applying a 180° pulse to the *other* single-quantum transition (b, c) as shown in Fig. 9. Such a selective pulse not only interchanges the populations in the

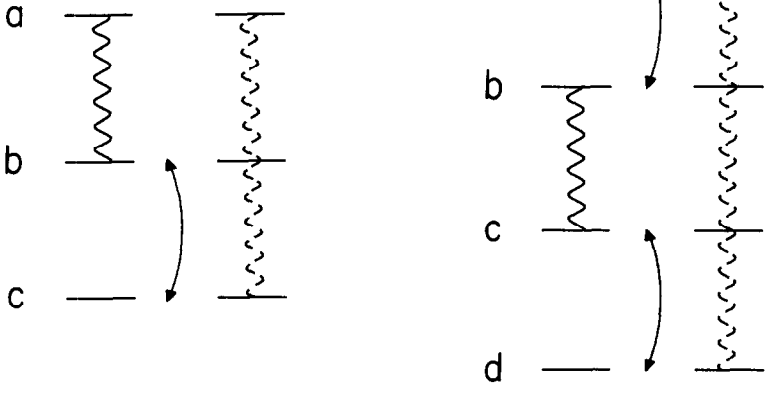

FIG. 9. In a three-level system (left), a single-quantum magnetization σ_{ab} can be excited by a 90° pulse at the frequency ω_{ab}. A subsequent 180° pulse applied at the ω_{bc} frequency swaps the indices b and c of all density matrix elements, converting σ_{ab} into double-quantum coherence σ_{ac}, as shown by Hatanaka, Terao and Hashi[51] in ^{27}Al. In a four-level system (right), a magnetization σ_{bc} can be generated by an initial 90° pulse, and converted into triple-quantum coherence σ_{ad} by applying simultaneous 180° pulses at the frequencies ω_{ab} and ω_{cd}, as demonstrated by Vega and Naor[56] in ^{23}Na.

levels b and c, but also swaps the indices b and c in all other density matrix elements.

This coherence transfer process had been predicted theoretically by Lu and Wood[54] who discussed 180° pulses in coherent optical spectroscopy. Hashi and co-workers[51] formulated the interconversion in terms of Bloch equations, which bear some similarity to those used by Brewer and Hahn[55] for optical systems. These transfer processes also lend themselves to an analysis based on single-transition operators, which will be briefly discussed in Section 4.10.

As in all double-quantum experiments, the time-evolution of the σ_{ac} coherence is interrupted after an interval t_1 by a monitoring pulse. This can be either a 180° pulse applied again to the (b,c) transition, to convert σ_{ac} back into σ_{ab}, or else a 180° pulse at the (a,b) frequency, which causes the double-quantum coherence σ_{ac} to transfer into σ_{bc}. In either case, the observable magnetization appears in a transition which is *not* subjected to an RF pulse, a behaviour which can be taken as proof of the existence of double-quantum coherence.

If all six energy levels of the ^{27}Al system shown in Fig. 8 were taken into consideration, any arbitrary coherence (say a five-quantum term between the $m = -5/2$ and $+5/2$ levels) could in principle be excited by an appropriate cascade of pulses. Clearly, some permutations of such a multi-step process are possible (since the first 90° pulse may be applied to any one of the allowed transitions) but the 180° pulses must affect neighbouring transitions in a consecutive manner. It should be remembered that the aim of the multiple-quantum experiment is the creation of a coherent superposition of states, and not a pumping process where the population of the ground state is transferred stepwise to higher energy levels.

4.4. *Modulated Pulses*

An interesting variation of the multi-step process has recently been described by Vega and Naor[56] to excite the triple-quantum coherence in the four energy-level system of ^{23}Na ($I = 3/2$) in a single crystal of sodium ammonium tartrate tetrahydrate. A 90° pulse is first applied to the central of the three allowed single-quantum transitions. The resulting transverse magnetization is then transferred to triple-quantum coherence by applying simultaneous 180° pulses to the allowed $(-3/2, -1/2)$ and $(+1/2, +3/2)$ "satellite" transitions, as shown schematically in Fig. 9. The selective 180° pulses are generated by modulating the RF carrier (which remains at the center frequency) with a modulation frequency matched to the quadrupolar splitting. The procedure may be further embellished by a preliminary enhancement of the population difference across the central transition, which can be achieved by applying another pair of selective 180° population inversion pulses to the satellites prior to the generation of transverse magnetization. The experiment is useful for the indirect detection of the single-quantum satellites, which can be quite broad if the quadrupolar splittings are not perfectly homogenous.[57,58] The triple-quantum precession frequency provides a way to measure the second-order quadrupole splitting.[56,58] A better understanding of the quadrupolar interaction may be relevant to the study of the mobility of sodium ions in such materials as β-alumina.[57]

4.5. *Heteronuclear Systems*

Systems of unlike spins I and S with scalar or dipolar couplings offer a fertile ground for multiple-quantum coherence transfer experiments. Stoll, Vega and Vaughan[59,60] have studied scalar-coupled proton–carbon pairs in isotropic solution with an experimental scheme known as "NMR interferometry". The proton magnetization of the IS system is first excited by a non-selective 90° pulse, whereupon a selective RF field is applied to one of the transitions of the ^{13}C doublet. If this irradiation were interrupted after a flip angle of 180°, a state of pure heteronuclear double- and zero-quantum coherence would result. Instead, Stoll *et al.* chose to use longer pulses with flip angles of 360° or 720°, which in effect return the coherence to the proton transitions where it can be detected like ordinary proton magnetization. The relevance of the experiment lies in its ability to determine the resonance frequency of the ^{13}C transitions with a sensitivity typical of proton NMR, in a manner reminiscent of INDOR spectroscopy.[24]

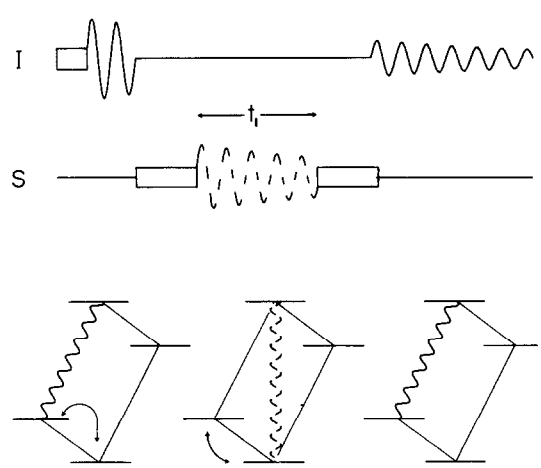

FIG. 10. A simple coherence transfer experiment in heteronuclear coupled systems. The energy level diagrams refer to a pair of spin-1/2 nuclei. A selective 90° pulse creates transverse magnetization in one of the I transitions, which is transferred into heteronuclear double-quantum coherence by a selective 180° pulse applied to one of the S transitions. The precession and transverse decay of the invisible coherence is measured by applying a second selective 180° S pulse after the evolution period to produce observable I magnetization.[59-61]

Since the coherence is continuously "stirred" and transferred back and forth between the allowed proton transitions and the zero- and double-quantum transitions, the transverse relaxation times will reflect an average of the T_2 values characteristic of these various coherences.[60]

A more satisfactory approach to heteronuclear systems has been demonstrated by Ernst,[61] who employed a selective 180° carbon pulse to transfer the proton magnetization to pure double-quantum coherence. In the evolution period t_1, this coherence is allowed to precess and decay in the absence of RF perturbation, to be subsequently transferred back to proton magnetization by another selective 180° ^{13}C pulse (Fig. 10). The sensitivity advantage of proton detection is retained, while the time constant of the transverse decay monitored in this two-dimensional experiment is truly characteristic of the heteronuclear double-quantum coherence. As will be discussed in Section 8, these relaxation times carry unique information about the correlation of the fluctuating fields at the sites of the nuclei S and I.

A technique proposed by Müller[49] represents a further step forward, because it employs strong pulses and does not require a detailed knowledge of the resonance frequencies. The method is particularly suitable for the indirect detection of the chemical shift of a spin S with an unfavourable gyromagnetic ratio by observing a more sensitive coupling partner I. The experiment shown in Fig. 11 uses a heteronuclear version of the double-pulse excitation (with simultaneous 180° pulses in the middle of the τ-delay). to excite both heteronuclear double- and zero-quantum coherence.

It can be shown that these coherences precess at frequencies $\Delta\omega_S \pm \Delta\omega_I$, which may at first sight appear inconvenient since the precession is determined by the offsets of both I and S nuclei in the two rotating frames. However, a 180° pulse in the middle of the evolution period interconverts the two coherences, leading to an average precession that depends only on the chemical shift $\Delta\omega_S$. A closely related scheme, which avoids multiple-quantum coherence but shares the sensitivity advantage of Müller's experiment, has been employed to detect ^{15}N and ^{199}Hg under conditions where direct detection would be difficult.[62,63]

The experiments due to Minoretti *et al.*[64] are suitable for partially oriented systems where the less sensitive nucleus S is subjected to a quadrupolar interaction. The double-quantum coherence may be excited by means of a two-pulse sequence applied to the S spins only, and transferred after an evolution period t_1 into observable proton magnetization by a 90° proton pulse. Here again, the motivation appears to be primarily the sensitivity advantage associated with proton NMR, since the information content is much the same as for a multiple-quantum experiment carried out on the S spins alone.

Henrichs and Schwartz[65,66] have described various coherence transfer processes induced in heteronuclear systems by selective pulses, with particular emphasis on the measurement of transverse relaxation in systems with degenerate transitions belonging to different irreducible representations of the symmetry group.

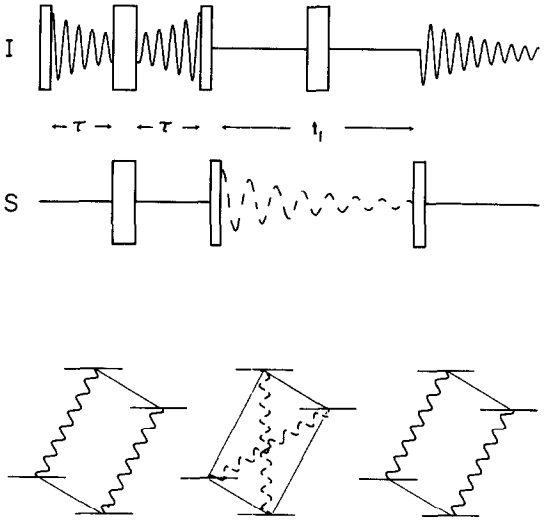

FIG. 11. Indirect detection of the chemical shift of a nucleus S with unfavourable gyromagnetic ratio. The single-quantum I magnetization is converted into heteronuclear zero- and double-quantum coherences, which are interconverted at the mid-point of the evolution period and transformed back into I magnetization for detection. (Redrawn after Müller.[49])

4.6. *Non-Equilibrium Systems*

An interesting variation of the selective pulse idea has been discussed by Aue, Bartholdi and Ernst,[47] who suggested that the initial thermal equilibrium could be perturbed by selectively inverting the populations across one of the transitions. The resulting "non-equilibrium of the first kind"[37] is then subjected to a non-selective 90° pulse. It can be shown[67] that all multiple-quantum coherences involving the same spin q which is flipped by the selective 180° pulse are excited uniformly by this method. This approach does not appear to have enjoyed much popularity so far, but its very simplicity suggests that the method should be part of the basic arsenal of any multiple-quantum spectroscopist. Since non-equilibrium population distributions may occur accidentally when a spin system has not been allowed to relax completely, it is quite conceivable that spurious multiple-quantum coherence could be created in this manner, causing interference phenomena in experiments that are not primarily concerned with multiple-quantum effects (see Section 9). Similar problems could arise in systems with chemically induced dynamic nuclear polarization.[37]

4.7. *Selective Multiple-Quantum Pulses*

In some systems, it is desirable to abandon the idea of non-selective pulses altogether and to opt for an entirely different approach which represents in some ways a continuation of CW multiple-quantum NMR. In the experiments described in Section 2, a continuous RF field is used to perturb the system, and p-quantum signals can be observed when the irradiation frequency equals a sub-multiple of the energy spacing between the eigenstates $\omega_{rs}^{p} = (E_s - E_r)/(p\hbar)$. Hatanaka and Hashi[68] have shown that it is possible to apply a pulse rather than a CW RF field to create multiple-quantum coherence σ_{rs}^{p} after the pulse is cut off. This phenomenon is directly analogous to the transient nutation of single-quantum magnetization about an RF pulse applied for a duration τ_p, which leads to a transverse magnetization component proportional to $\sin \gamma B_1 \tau_p$. In the case of an oriented spin $I = 1$, which has been the subject of a detailed study by Vega and Pines,[42] a weak RF pulse applied at the centre of the quadrupolar doublet causes the double-quantum coherence to nutate with a frequency

$$\omega_{\text{eff}} = \frac{(\gamma B_1)^2}{\omega_Q} = \frac{\omega_1^2}{\omega_Q}. \tag{17}$$

In comparison to the nutation of single-quantum coherence, the effective RF field appears attenuated by a factor ω_1/ω_Q. Thus, for a pulse width τ_p, the flip angle $\alpha = \omega_{\text{eff}}\tau_p$ is a function of the quadrupolar splitting, and the magnitude of the double-quantum coherence varies across a powder pattern.

The double-quantum nutation could be observed in Hashi's ^{27}Al system both by monitoring the double-quantum coherence in the usual manner, as well as by observing the "stirring" of the populations of levels a and c in Fig. 8 induced by applying the RF field half-way between the allowed transitions (a,b) and (b,c).[68] Both Vega[69] and Wokaun and Ernst[70] have discussed extensions of the selective multiple-quantum pulses to oriented $I = 3/2$ systems and to coupled $I = 1/2$ spins. It should be noted that the effective nutation frequency varies from case to case: for example, the double-quantum coherence in $I = 3/2$ systems nutates with a frequency

$$\omega_{\text{eff}} = \frac{7}{4}\frac{\omega_1^2}{\omega_Q} \tag{18}$$

whereas the nutation of the triple-quantum coherence in the same spin system depends on the third power of the RF field

$$\omega_{\text{eff}} = \frac{3}{8}\frac{\omega_1^3}{\omega_Q^2}. \tag{19}$$

Not surprisingly, double-quantum coherence can only be associated with a pair of spin 1/2 nuclei if the scalar or dipolar coupling is not vanishingly small. This circumstance is reflected in the effective nutation frequency

$$\omega_{\text{eff}} = \frac{8\pi J \omega_1^2}{(\omega_A - \omega_B)^2}. \tag{20}$$

In each case, the RF pulse is assumed to be short on the time scale of the transverse relaxation of the system. Clearly, inherently small nutation frequencies will make it difficult to generate any substantial multiple-quantum coherence because longer pulses cannot successfully compete with the effects of relaxation. This problem tends to be critical in ^{23}Na for example, where the size of the quadrupolar coupling is such that Vega and Naor[56] were forced to abandon selective multiple-quantum pulses to turn to modulated pulses.

Selective double-quantum pulses have been used extensively by Pines and co-workers in deuterium NMR, both in single crystal studies and polycrystalline powders.[42,50] Selective pulses tend to excite a subgroup of all possible multiple-quantum coherences. In the case of coupled deuterons for example, selective pulses will generate only those double-quantum terms whose precession frequencies are independent of the quadrupolar interaction, in contrast to the double-pulse excitation which generates additional coherences that tend to complicate the spectra.[71,72]

4.8. *Multiple-Quantum Cross-Polarization*

The modest sensitivity of nuclei with low gyromagnetic ratios can often be overcome to some extent if there is a coupling to a neighbouring nucleus with a more favourable γ. The classic experiment due to Hartmann and Hahn[73] establishes a contact between the nuclei S and I by matching the nutation frequencies of their magnetization about their respective RF fields

$$\gamma_I B_I = \gamma_S B_S. \tag{21}$$

Cross-polarization methods have found widespread applications in solid-state experiments[74] and more recently in isotropic solutions[75,76] where the scalar interaction provides a vehicle for the transfer of the polarization. In systems where the S spins are subject to quadrupolar splittings, the coherence transfer experiment is often arranged to enhance only one of the allowed S spin transitions, which can be treated as a fictitious spin 1/2 transition. In ^{14}N ($S = 1$) for example,[52,53] only one of the allowed transitions can normally be irradiated because of the magnitude of the quadrupole splitting. In this situation, a modified Hartmann–Hahn condition must be fulfilled which, incidentally, in no way impairs the efficiency of the cross-polarization experiment:

$$\gamma_I B_I = \sqrt{2}\gamma_S B_S. \tag{22}$$

An entirely different approach to IS systems with $S = 1$ is based on the idea that the double-quantum transition of the S-spin can also behave as a fictitious spin 1/2.[77–79] In order to establish a Hartmann–

Hahn contact between the I (proton) magnetization and the S double-quantum transition, it is necessary to fulfill the requirement[78]

$$\gamma_I B_I = \frac{(\gamma_S B_S)^2}{\omega_Q} \tag{23}$$

It should be noted that the transfer depends on ω_Q and cannot be uniformly efficient across the entire width of a powder pattern. The double-quantum coherence created in this manner may be allowed to evolve for a time t_1 in order to characterize the chemical shift of the S spins, prior to a second transfer back to observable magnetization by another suitable Hartmann–Hahn contact. This approach, which can be carried out in the manner of a two-dimensional experiment,[79] allows the detection of the less sensitive S spins with the full sensitivity of proton NMR, not unlike Müller's method for isotropic solutions.[49]

If the proton spectrum itself presents detection problems because of extensive homonuclear dipolar interactions, it may be preferable to convert the double-quantum coherence into observable S-spin magnetization. This can be achieved by a non-selective 90° pulse which must be shifted in phase through 45°.[78] A third method avoids the detection of the double-quantum coherence altogether and simply monitors the destruction of the spin-locked proton magnetization due to the Hartmann–Hahn transfer.[78,80] A variation of these experiments circumvents the search for the resonance condition by reducing the proton spin-locking field gradually to zero prior to the application of the RF field at the S spin double-quantum frequency,[78,81] in the manner of an adiabatic demagnetization in the rotating frame. A simple extension of any cross-polarization experiment can be made to measure the $T_{1\rho}$ relaxation time of the double-quantum coherence when the latter is maintained in a spin-locked condition after the transfer of coherence.[78]

4.9. *Selective Excitation of Coherence of Specified Order*

The number of multiple-quantum transitions tends to grow rapidly in larger spin systems. To simplify the interpretation, it is desirable to focus the attention on transitions of a given order, for example on the quadruple-quantum transitions alone. Broadband excitation techniques, such as the double-pulse method, tend to create coherences between all pairs of eigenstates, a situation where the order of the system is said to be spread over the entire density matrix.[41] Although it is possible to restrict the detection to a specified order p, as is shown in Section 5, it is in principle more efficient to avoid the excitation of undesired coherences in the first place by transferring the order selectively to those multiple-quantum transitions that one actually wishes to observe.

If the basic $90°$–τ–$90°$ sequence is applied to a pair of coupled deuterons,[72] explicit density matrix calculations of the coherence transfer reveal that the odd and even orders are proportional to $\sin \Delta\omega\tau$ and $\cos \Delta\omega\tau$ respectively. It follows that the $90°_x$–$\tau/2$–$180°_x$–$\tau/2$–$90°_x$ sequence (the subscripts indicate that all pulses are applied along the x-axis of the rotating frame) specifically excites only *even* quantum coherence, since the offset term $\Delta\omega\tau$ is cancelled just before the last 90° pulse. However, if the third pulse is applied along the y-axis, the system behaves as under the influence of an offset $\Delta\omega\tau = \pi/2$. This is unfavourable for the even orders and leads to the selective excitation of the odd-quantum coherences. This turns out to be a general symmetry property and has been successfully applied in dipolar-coupled proton systems in oriented benzene.[50]

A more involved approach has been described recently by Warren *et al.*,[82] who used a sophisticated sequence of pulse packages, each burst being shifted in phase through an angle $\phi = 2\pi/p$ to achieve the selective excitation of p-quantum coherence. Preliminary results indicate that good selectivity can be obtained, and the technique is more efficient than selective detection used in conjunction with broad-band excitation, provided the dipolar or scalar splittings are well resolved in the single-quantum spectrum.

4.10. *Single Transition Operators*

So far, this discussion of multiple-quantum excitation has been pursued with little reference to any mathematical treatment. The widely accepted approach is based on single-transition operators, which were introduced by Vega and Pines[42] and subsequently recast in more general terms by both Vega[69] and Wokaun and Ernst.[70]

Consider a system with an arbitrary number of eigenstates N, where the attention is focussed on a particular pair of eigenstates ψ_r and ψ_s regardless whether such a pair spans an allowed transition or an arbitrary multiple-quantum transition. It is always possible to define a set of three spin operators for each transition, which can be represented by a set of three Pauli-matrices. For example, each of the three transitions in the $I = 1$ spin system requires three operators whose matrix representations are shown in Table 1. The first two rows of matrices correspond to the allowed transitions $(-1, 0)$ and $(0, +1)$, while the third row of matrices in Table 1 represents the double-quantum transition $(-1, +1)$. Each row in effect represents a fictitious spin 1/2, since the third state is not involved. Larger spin systems require a trivial extension of the dimensions of these matrices by including additional rows and columns of zeroes for the eigenstates that are not involved in the particular transitions.

Within each fictitious spin 1/2 system, the set of

TABLE 1. Matrix representations of single-transition operators for $I = 1$

$$I_x^{1-2} = \frac{1}{2}\begin{pmatrix} 0 & 1 & 0 \\ 1 & 0 & 0 \\ 0 & 0 & 0 \end{pmatrix}; \quad I_y^{1-2} = \frac{i}{2}\begin{pmatrix} 0 & -1 & 0 \\ +1 & 0 & 0 \\ 0 & 0 & 0 \end{pmatrix}; \quad I_z^{1-2} = \frac{1}{2}\begin{pmatrix} 1 & 0 & 0 \\ 0 & -1 & 0 \\ 0 & 0 & 0 \end{pmatrix};$$

$$I_x^{2-3} = \frac{1}{2}\begin{pmatrix} 0 & 0 & 0 \\ 0 & 0 & 1 \\ 0 & 1 & 0 \end{pmatrix}; \quad I_y^{2-3} = \frac{i}{2}\begin{pmatrix} 0 & 0 & 0 \\ 0 & 0 & -1 \\ 0 & +1 & 0 \end{pmatrix}; \quad I_z^{2-3} = \frac{1}{2}\begin{pmatrix} 0 & 0 & 0 \\ 0 & 1 & 0 \\ 0 & 0 & -1 \end{pmatrix};$$

$$I_x^{1-3} = \frac{1}{2}\begin{pmatrix} 0 & 0 & 1 \\ 0 & 0 & 0 \\ 1 & 0 & 0 \end{pmatrix}; \quad I_y^{1-3} = \frac{i}{2}\begin{pmatrix} 0 & 0 & -1 \\ 0 & 0 & 0 \\ +1 & 0 & 0 \end{pmatrix}; \quad I_z^{1-3} = \frac{1}{2}\begin{pmatrix} 1 & 0 & 0 \\ 0 & 0 & 0 \\ 0 & 0 & -1 \end{pmatrix}.$$

operators obeys the usual commutation relationship

$$[I_z^{r-s}, I_y^{r-s}] = iI_x^{r-s} \tag{24}$$

and cyclic permutations. This equation describes the familiar nutation of a longitudinal magnetization I_z^{r-s} about an RF field applied to the (r,s) transition along the y-axis of the rotating frame, the flip angle being represented by θ:

$$\exp\{-i\theta I_y^{r-s}\} I_z^{r-s} \exp\{+i\theta I_y^{r-s}\} = I_z^{r-s}\cos\theta + I_x^{r-s}\sin\theta. \tag{25}$$

The result of this nutation is a pure x-magnetization I_x^{r-s} for $\theta = 90°$. Modified commutation relationships are applicable when *three* different states ψ_r, ψ_s and ψ_t are involved, for example

$$[I_x^{t-s}, I_x^{r-t}] = \frac{i}{2} I_y^{s-r}. \tag{26}$$

Various combinations of x, y and z components lead to different commutators.[69,70] According to equation (26), a magnetization I_x^{t-s} is transformed into I_y^{s-r} by the application of an x-pulse to the (r,t) transition:

$$\exp\{-i\theta I_x^{r-t}\} I_x^{t-s} \exp\{+i\theta I_x^{r-t}\} = I_x^{t-s}\cos\frac{\theta}{2} + I_y^{s-r}\sin\frac{\theta}{2}. \tag{27}$$

Note that, as a result of the factor 1/2 in equation (26), a complete transfer of the (t,s) magnetization into (r,s) coherence is achieved by applying a 180° pulse to the (r,t) transition. This describes a typical "multi-step process"[54] as it has been used in ^{27}Al as well as in ^{23}Na triple-quantum NMR. A remarkable consequence of the factor 1/2 in equation (26) is the fact that a spin system does not return to its initial state after a 360° pulse, but requires a pulse with a flip angle of 720° if the algebraic sign of the coherence is not to be reversed. This is in agreement with the observations of Vaughan and co-workers.[59,60] Stoll, Wolff and Mehring[83,84,85] have studied extensively this so-called "spinor character" in deuterium NMR, both for single- as well as for double-quantum transitions.

Single transition operators have found widespread applications in the description of selective multiple-quantum pulses. In the case of an oriented spin 1 subject to quadrupolar interaction, the Hamiltonian in the rotating frame has the form

$$\mathcal{H} = -\Delta\omega I_z + \tfrac{1}{3}\omega_Q[3I_z^2 - I(I+1)] - \omega_1 I_x. \tag{28}$$

This equation can be translated into single-transition operators by appropriate substitutions:

$$I_z = I_z^{1-2} + I_z^{2-3} + I_z^{1-3} = 2I_z^{1-3} \tag{29}$$

$$I_x = \sqrt{2}[I_x^{1-2} + I_x^{2-3}] \tag{30}$$

to yield the equivalent Hamiltonian

$$\mathcal{H} = -2\Delta\omega I_z^{1-3} + \frac{2\omega_Q}{3}[I_z^{1-2} - I_z^{2-3}] - \sqrt{2}\omega_1[I_x^{1-2} + I_x^{2-3}]. \tag{31}$$

It turns out[69,70] that this modified Hamiltonian can be diagonalized analytically for an arbitrary ratio ω_1/ω_Q. In effect, a selective pulse with $\omega_1 \ll \omega_Q$ and $\Delta\omega = 0$ causes the longitudinal magnetization to be transferred directly into double-quantum coherence

$$\exp\{-i\mathcal{H}\tau_p\} I_z^{1-3} \exp\{+i\mathcal{H}\tau_p\} = I_z^{1-3}\cos\frac{\omega_1^2}{\omega_Q}\tau_p + I_x^{1-3}\sin\frac{\omega_1^2}{\omega_Q}\tau_p. \tag{32}$$

This equation (except for the nutation frequency $\omega_{\text{eff}} = \omega_1^2/\omega_Q$) is directly analogous to equation (25) and highlights the resemblance between selective single- and multiple-quantum pulses.

5. DETECTION TECHNIQUES

The basic pulse experiment described in Section 3 illustrates the inherent symmetry of the time domain experiment: the second excitation pulse transfers the allowed magnetization into multiple-quantum coherence, and the monitoring pulse simply reverses this transformation. Because of this, the detection techniques closely parallel the various excitation methods. After the resurrection of the observable magnetization by the monitoring pulse, one can detect either the complete free induction decay, or else only a single data point at some time after the monitoring pulse.

5.1. *Pulses and Echoes*

In most homonuclear systems, a simple 90° pulse suffices to ensure an efficient coherence transfer,

regardless of the type of excitation that may be selected. Problems may arise however if the single-quantum magnetization dephases very rapidly under the influence of, say, a large inhomogeneous quadrupolar interaction. This situation arises in deuterium NMR of polycrystalline samples or non-oriented liquid crystals, where the signal tends to decay before the receiver has recovered. In ordinary one-dimensional deuterium NMR, this problem is usually circumvented by generating a quadrupolar echo with a 90°_x–τ–90°_y–τ–acquisition sequence.[86] The signal observed in this manner corresponds in principle to the hypothetical free induction decay that would be recorded if the receiver were activated immediately after the first pulse, although the amplitude is attenuated since the quadrupolar dephasing is only partly reversed by the second 90° pulse. The double-quantum work on deuterium by the Berkeley group[42,50,77] makes extensive use of quadrupolar echoes. All four sequences in Fig. 12 assume selective multiple-quantum excitation, although the same detection methods are compatible with alternative excitation techniques. The P_2 pulse in Fig. 12B acts as

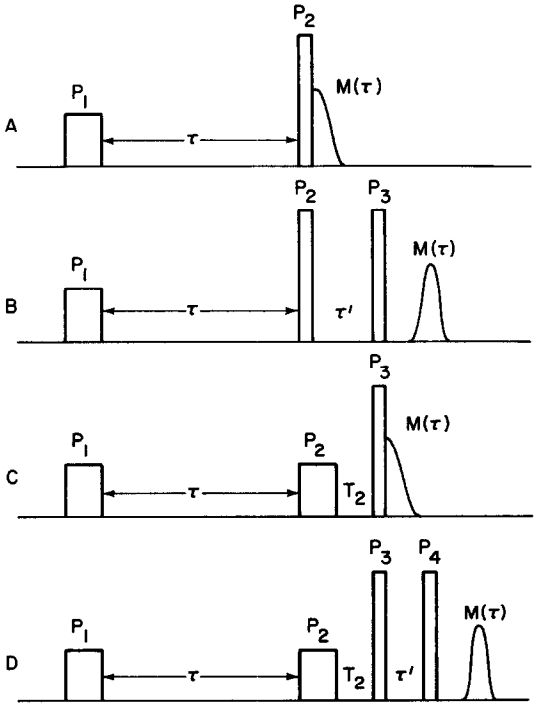

FIG. 12. Variations on the theme of monitoring pulses. The multiple-quantum coherence evolving in the evolution period τ is either converted into transverse single-quantum magnetization by a strong 90° pulse (A and B) or stored in the form of population differences by means of a selective multiple-quantum pulse (C and D). The resulting non-equilibrium populations are converted into observable magnetization by a strong 90° pulse. In either scheme, the single-quantum magnetization can be refocussed by a 90° pulse to overcome receiver dead-time problems (B and D). Reproduced from reference 50.

monitoring pulse to transfer the invisible coherence, while the P_3 pulse operates on the single-quantum magnetization to generate a quadrupolar echo. The delay τ' in the echo sequence is adjusted to suit the recovery characteristics of the receiver and does not affect the multiple-quantum experiment.

An alternative approach avoids the use of a non-selective coherence transfer pulse. Instead, a "storage pulse" is employed to transfer the invisible coherence back into diagonal elements of the density matrix, thereby reversing the effect of a selective double-quantum excitation pulse.[42,64,68] An ordinary 90° observation pulse is then applied to transfer the population differences into single-quantum coherence (Fig. 12C). The abnormal signal amplitudes of the spectrum obtained in this manner betray the non-equilibrium population distribution. This approach can be embellished with a quadrupolar echo to avoid receiver recovery problems in powder spectra (Fig. 12D). Hatanaka and Hashi[68] have shown that the information stored in this manner can be retrieved much later, provided the T_2 delays in Fig. 12 are short on the time scale of the spin–lattice relaxation. In systems with very large quadrupole splittings, where selective single-quantum pulses offer the most convenient means of excitation, the same type of pulses may be used to monitor multiple-quantum coherence. Thus the invisible coherence σ_{ac} in Hashi's ^{27}Al system (Fig. 9) can be converted into visible magnetization σ_{ab} simply by applying a selective 180° pulse to the allowed (b, c) transition.[51]

In heteronuclear systems, other detection schemes must be used to reverse the effect of the excitation sequences.[49,61] Minoretti *et al.*[64] have given a detailed discussion of the transfer of multiple-quantum coherence in heteronuclear systems. Various combinations of selective and non-selective pulses can be employed, particularly in systems where the double-quantum coherence of a partially oriented quadrupolar nucleus S can be transferred to the allowed transitions of a spin-1/2 coupling partner I. The latter's magnetization does not suffer from quadrupolar broadening and may be detected with enhanced sensitivity if $\gamma_I/\gamma_S > 1$.

Most authors have limited the discussion of these experiments to ideal pulses, although off-resonance effects[60] and flip angles which depart from 90°[72,64] can introduce severe amplitude and phase anomalies.

5.2. *Two-dimensional Fourier Transformation*

Even in its modern, pulsed incarnation, multiple-quantum NMR need not involve any Fourier transformation at all. In simple cases, the evolution of the multiple-quantum coherence can be mapped out in the t_1 domain, and both the precession frequency and the transverse decay can be measured from the damped cosinusoidal t_1-dependence of the signals recorded after the monitoring pulse.[41,51] In conventional NMR, this would be equivalent to

measuring resonance frequencies and linewidths by inspection of the free induction decay. Not surprisingly, most authors agree that a Fourier transformation with respect to t_1 is quite helpful, both to improve the sensitivity and to unravel a manifold of frequencies.[87] The raw data for this Fourier transformation is obtained by incrementing t_1 in regular intervals, much like the sampling of a free induction decay signal. If the frequency domain lineshapes are to provide an undistorted picture of the transverse relaxation, t_1 must be sampled until the multiple-quantum signals have decayed completely. This latter requirement tends to make multiple-quantum experiments rather time-consuming, since the information obtained for longer t_1 values contributes little to the overall signal-to-noise ratio of the frequency-domain multiple-quantum spectrum.[88] Because the t_1 evolution can only be mapped out step by step, the experiment must be started all over again for each t_1 value. In this sense, multiple-quantum spectroscopy is part of the growing field of two-dimensional NMR spectroscopy. Since the most cumbersome aspect consists in sampling the t_1 domain, there is no significant addition to the spectroscopist's burden if the free induction decays observed after the monitoring pulse are recorded in full length as a function of the running time parameter t_2. In this manner, a complete matrix $S(t_1, t_2)$ is obtained which can be transformed into a two-dimensional frequency spectrum $S(F_1, F_2)$.[47,89] A typical example is shown in Fig. 13, where the $F_1 = \omega_1/(2\pi)$ dimension shows the multiple-quantum precession frequencies, while the $F_2 = \omega_2/(2\pi)$ domain is reserved for the ordinary spectrum of allowed transitions, obtained by Fourier transformation of the signals observed after the monitoring pulse.

To avoid overloading the data storage system, it is sufficient to retain only the peaks in the F_2 domain and store these as a function of t_1, thus discarding the vast number of data points that make up the plains and valleys in the two-dimensional landscape.

If one chooses to neglect the advantage of the Fourier transform in the F_2 domain for the sake of simplified data handling, one or more acquisition points may be selected at some time after the monitoring pulse. The timing is not entirely trivial, since the free induction decays often start with a zero-crossing point, because the single-quantum magnetization vectors resurrected by a non-selective monitoring pulse begin their precession with opposite phases. In the case of the partially oriented spin 1 illustrated in Fig. 6, the F_2 frequency domain does indeed reveal two signals with opposite phases. Clearly, the integral of the frequency domain vanishes, and it follows from one of Fourier's basic theorems that the initial value of the free induction decay also vanishes.[90] If a single point is to be taken in this case, it should be at a time τ after the monitoring pulse. The best τ-interval is equal to the delay required for the most efficient double-pulse excitation. A 180° pulse may be inserted in the middle of this τ-interval to remove the effect of the chemical shift.[62,64] In deuterium powder patterns, no single acquisition point can provide satisfactory information for all crystallite orientations.

The multiple-quantum modulation is often similar

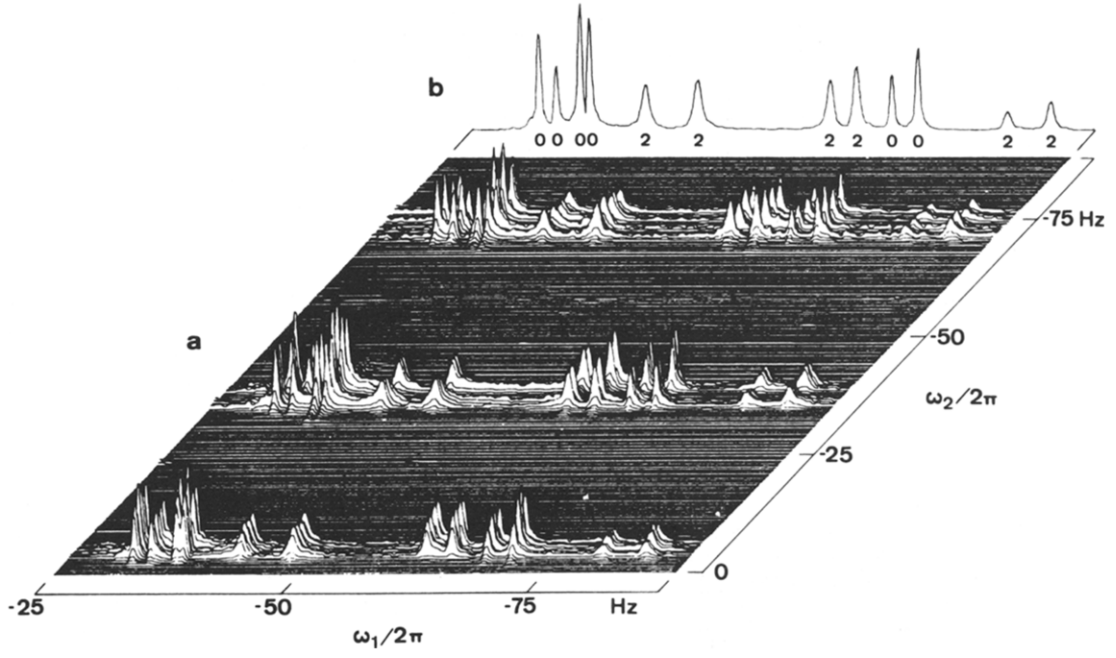

FIG. 13. Two-dimensional representation of the high-resolution multiple-quantum spectrum of the three aromatic protons in 2-furancarboxylic acid methyl ester. The ω_1-domain contains the 6 zero- and 6 double-quantum signals, the single- and triple-quantum transitions being suppressed by a phase-cycling technique. Reproduced from Wokaun and Ernst.[45]

for the various peaks in the F_2 domain, and the presentation of the information in the form of a two-dimensional spectrum may be highly redundant, as can be seen in Fig. 13, where the F_1 frequencies are the same throughout the two-dimensional map. It is possible to project the two-dimensional spectrum to collapse the F_2 domain.[91] To prevent the cancellation of signals with opposite algebraic signs, it is necessary to calculate the absolute-value spectrum before integration. Alternatively, it is possible to improve the signal-to-noise ratio by calculating the power spectrum and by taking the square root after the integration over F_2.[67] In experiments where selective pulses are employed to monitor the invisible coherence,[64] no such precautions are necessary because the signals do not appear with opposite phases.

In many systems, however, the separation of multiple-quantum information achieved by spreading the spectra into two orthogonal frequency domains can be quite instructive. In symmetrical systems, the single-quantum resonances appearing in the F_2 domain can be classified according to the irreducible representations of the symmetry group of the spin system. In this case, the multiple-quantum signals will be separated accordingly since the monitoring pulse cannot break the symmetry, and all coherence transfer processes are necessarily confined within the irreducible representations. This circumstance greatly simplifies the double-quantum spectra in systems with equivalent coupled deuterons.[72] In the partially deuterated liquid crystals studied by Hsi, Zimmermann and Luz,[92] the F_2 axis separates deuterium signals originating from different CD_2 groups in the alkoxy chains because of the spread in quadrupolar splittings.

It should be emphasized that multiple-quantum spectroscopy bears a very close analogy to heteronuclear two-dimensional NMR, a method which has been introduced by Maudsley and Ernst.[93] Both the heteronuclear and the multiple-quantum techniques are concerned with the indirect detection of coherence. In the former case however, the coherence that one wishes to monitor corresponds to ordinary single-quantum magnetization, which cannot be observed directly simply because the precession frequencies lie outside the bandwidth of the receiver, thus requiring a transfer of coherence to become accessible.

5.3. *Selective Detection*

It has been assumed so far that the coherence transfer processes behave ideally according to the theoretical equations. In actual practice however, the initial excitation rarely generates pure multiple-quantum coherence, but usually produces a sizeable amount of spurious single-quantum magnetization. The monitoring pulse will leave some of this magnetization in the transverse plane, and can also excite an additional free induction signal that is alien to the multiple-quantum experiment and simply stems from the fact that the population differences may have partly recovered at the end of the evolution period. Such imperfections can easily obscure multiple-quantum spectra if they are not removed in some way. Fortunately, a p-quantum coherence has a characteristic response to a phase shift ϕ of the RF pulses used for the excitation

$$\sigma^p(\phi) = \sigma^p(o) \exp\{-ip\phi\}. \quad (33)$$

This property can be used to ensure that the desired multiple-quantum signal is distinguished from the background of artifacts. For $p = 2$ it is sufficient to add and subtract four different transients while the excitation phase is advanced in increments of 90° to cause the double-quantum signal to alternate in sign.[40] This technique was used in the deuterium spectra shown in Fig. 6. A simpler scheme relies on the addition of two transients which differ by a 180° phase shift, a procedure which retains all even orders p, as can be seen in Fig. 13. Such schemes can be extended to any desired order p, provided the RF phase can be advanced in increments of $\Delta\phi = 180°/p$.[94] Note that a sequence appropriate for $p = 2$ also allows the detection of $p = 6$, and phase increments of 60° allow both $p = 3$ and $p = 9$ to be observed.[45] Such schemes can greatly simplify the task of optimizing the multiple-quantum excitation, since the signal observed after the first Fourier transform for $t_1 = 0$ is directly proportional to the magnitude of the invisible coherence of order p.

Wokaun and Ernst[45] have proposed a more sophisticated approach, which requires $2N$ different two-dimensional experiments for systems where the highest possible order is an N-quantum transition. The $2N$ experiments differ in the excitation phase $\phi_q = \pi q/N$ $(q = 0, 1 \ldots 2N-1)$ and, after a two-dimensional Fourier transform, the $2N$ matrices $S(F_1, F_2, \phi_q)$ must be stored separately. The selection of a p-quantum spectrum is achieved by linear combinations which amount to a Fourier analysis with respect to the phase ϕ:

$$S^p(F_1, F_2) = \frac{1}{N} \sum_{q=0}^{2N-1} S(F_1, F_2, \phi_q) \cos(p\phi_q). \quad (34)$$

This approach is obviously quite powerful, since any multiple-quantum spectrum of desired order p can be extracted from the same basic set of experiments. On the other hand, one cannot easily determine whether a given p-quantum coherence has been successfully excited before the entire set of N two-dimensional experiments has been completed.

A completely different technique for selective detection has been proposed by Bax *et al.*[95] who used pulsed field gradients to distinguish different orders of multiple-quantum coherence.

6. SIMPLIFICATION OF SPECTRAL INFORMATION

Although the bewildering array of techniques re-

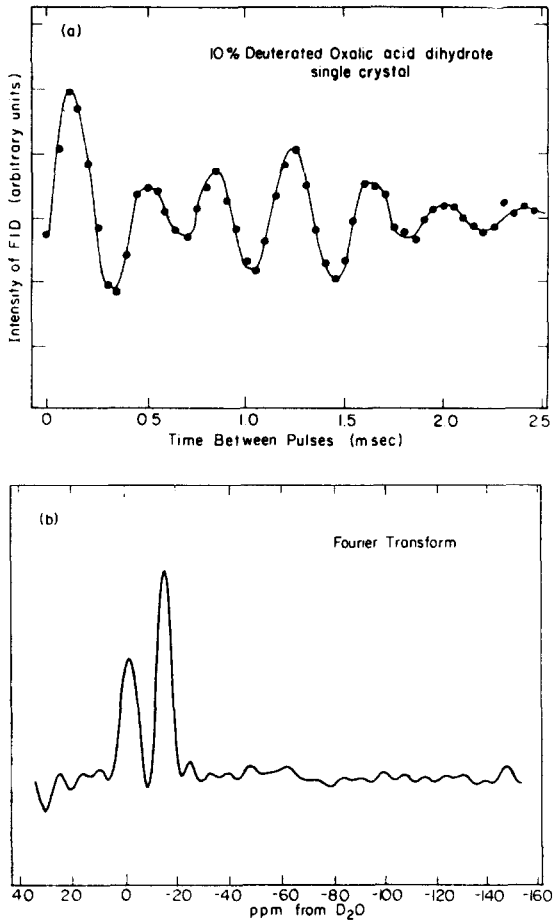

FIG. 14. Double-quantum "interferogram" (top) and spectrum (below) of deuterium in a single crystal of 10% deuterated oxalic acid dihydrate, obtained in the presence of proton decoupling. The signals arising from the carboxyl (right) and the hydrate (left) deuterons are well resolved in the double-quantum spectrum, although they cannot be separated in either proton or single-quantum deuterium spectra. (Vega, Shattuck and Pines.[96])

viewed in the preceding chapters may at first sight appear to lack in justification, multiple-quantum NMR can provide a great deal of novel information, particularly in spin systems which present difficulties in conventional single-quantum NMR.

6.1. *Quadrupolar Nuclei*

Spin systems with $I \geqq 1$ in single crystals, powders and liquid crystals have been the object of extensive NMR studies. The ordinary single-quantum spectra are dominated by the quadrupolar interaction, which leads to splittings that may vary from a few hertz in partially ordered deuterium systems to several megahertz in rigid lattices containing ^{14}N. The determination of quadrupole tensors with respect to the molecular frame reveals a correlation between the electric field gradients and the chemical structure, a type of information that may be complementary to the chemical shift. Unfortunately, the sheer magnitude of the quadrupolar interaction often obscures the chemical shifts. The quadrupolar Hamiltonian is expressed to first order by

$$\mathscr{H}^{(1)} = \tfrac{1}{3}\omega_Q[3I_z^2 - I(I+1)] \qquad (35)$$

and has the effect of shifting the upper and lower eigenstates of a spin 1 by the same amount, as shown in Fig. 4. As a result, the precession frequency of the double-quantum coherence is independent to first order of the quadrupole interaction, and provides a direct measure of the chemical shift. This property can be exploited in single crystals of deuterated materials, where the double-quantum transitions belonging to non-equivalent deuterium nuclei can be readily resolved, as Vega *et al.*[96] demonstrated in a crystal of partially deuterated oxalic acid dihydrate (Fig. 14).

The chemical shift anisotropy can be determined by rotating the crystal with respect to the static field.[96] The orientation of the tensor with respect to the molecular frame can be determined in this manner, provided the crystal structure is known from X-ray or neutron diffraction studies. Alternatively, it is possible to perform a double-quantum experiment on a polycrystalline powder. The spectrum obtained from the double-quantum transition resembles the conventional powder spectrum of a true spin 1/2 and provides a direct measure of the chemical shift anisotropy. An example is shown in Fig. 15, which represents the double-quantum spectrum of deuterated benzene.[50] The width of the powder pattern determined in this manner is far too small to be measured directly from the single-quantum spectrum, where the chemical shift is convoluted with

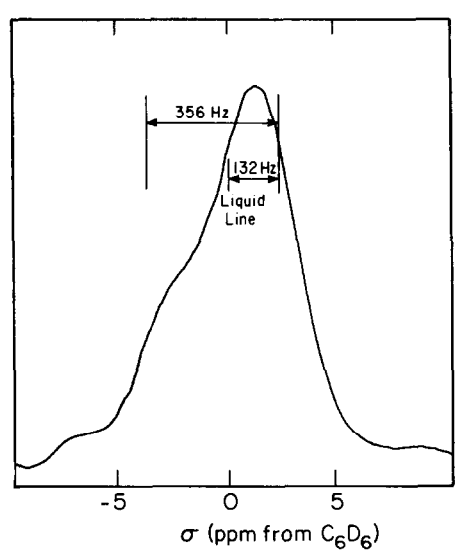

FIG. 15. Deuterium double-quantum powder spectrum of mono-deuterated benzene diluted in 90% normal benzene, obtained at −40°C in the presence of proton decoupling. The spectrum reveals a typical pattern due to the anisotropy of the chemical shift, somewhat distorted because of the difficulty of achieving uniform excitation and detection of double-quantum coherence for all crystallites. Reproduced from reference 50.

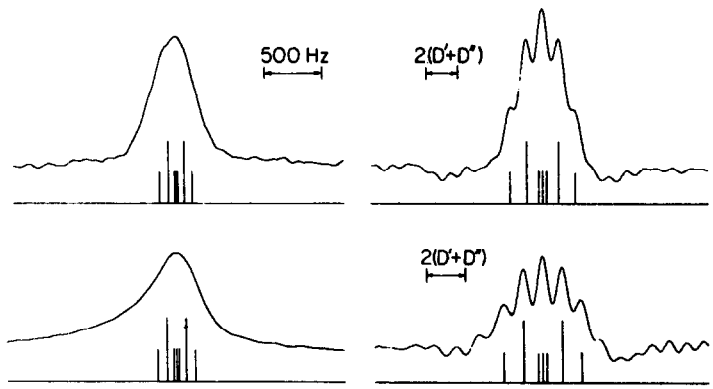

FIG. 16. Single-quantum spectra (left) and double-quantum spectra (right) of deuterium in selectively deuterated oriented *p*-pentoxybenzylidene-*p*-heptylaniline (50.7), obtained in the presence of proton decoupling at 57°C (top) and 41°C (below). The dipolar fine structure is obscured in the ordinary spectrum by quadrupolar broadening, but can be readily resolved in the double-quantum spectrum. (Hsi, Zimmermann and Luz.[92])

the quadrupolar splitting to form a broad powder pattern.

By combining deuterium double-quantum NMR with magic angle spinning,[147] it is possible to eliminate the anisotropy of the chemical shift and measure the isotropic shift in polycrystalline powders. (The width of the single-quantum powder spectrum makes the use of conventional magic angle spinning difficult.)

Since the chemical shifts of deuterons and protons are directly proportional, the double-quantum spectra provide an indirect measure of the chemical shift anisotropy in homologous proton-substituted systems. This information cannot be readily obtained from the normal proton spectrum, because the homonuclear dipolar interactions obscure the chemical shift. It is possible however to observe the NMR spectra of the residual protons in incompletely deuterated samples under conditions of deuterium decoupling (see Section 6.4.).

In the presence of homonuclear couplings among the deuterons, the double-quantum deuterium spectra no longer provide a straightforward measure of the chemical shift. In systems with two magnetically equivalent deuterons,[71] only two of the six double-quantum transitions are determined by the shift alone (so-called coherences of class 1[72]). Two further double-quantum frequencies depend on the dipolar interaction (class 2), while the remaining two, which can be readily excited with the double-pulse sequence, are affected by the quadrupole splitting (class 3).

Hsi, Zimmermann and Luz[92] have employed double-quantum deuterium NMR to resolve homonuclear dipolar couplings in liquid crystalline systems. In *p*-pentoxybenzylidene-*p*-heptylaniline (commonly referred to as 50.7), two protons in the α position and one in the γ position of the pentoxy group were selectively replaced by deuterium. In the presence of proton decoupling, the γ double-quantum deuterium spectra show a dipolar fine structure due to the long-range coupling to the α deuterons (right-hand side in Fig. 16), which cannot be resolved in the

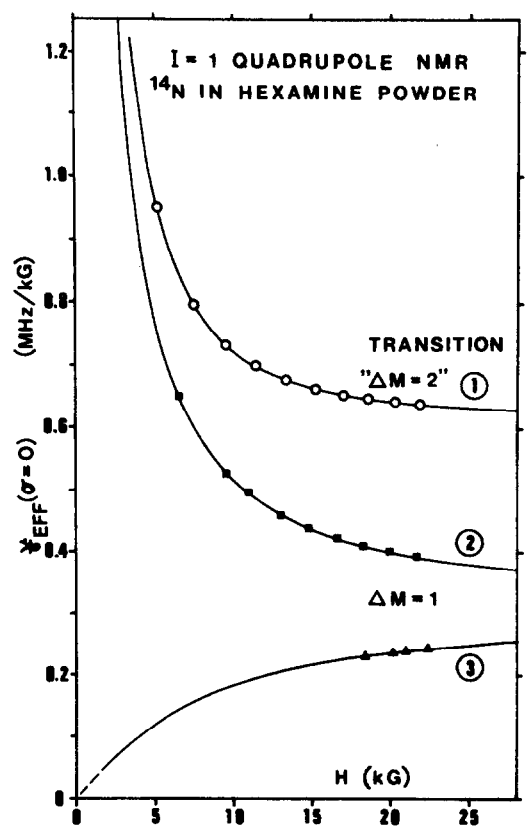

FIG. 17. The CW NMR spectrum of ^{14}N in polycrystalline $N_4(CH_2)_6$ shows the usual $(-1,0)$ and $(0,+1)$ transitions (the "edges" of the powder pattern are indicated by filled symbols). In addition, the $(-1,+1)$ transition is partly allowed in the single-quantum spectrum at low field (open symbols). A two-photon double-quantum absorption would appear at half the frequency shown for $\Delta m = 2$, and would appear half-way between the single-quantum transitions in the limit of high field only. The effective gyromagnetic ratios $\gamma = \nu/B_0$ of all transitions would be field-independent if the quadrupole interaction could be treated to first order only.

ordinary deuterium spectrum because of quadrupolar broadening.

For $I = 1$ nuclei with very large quadrupole interactions, the second order quadrupole splitting should not be ignored. The additional term in the Hamiltonian[97]

$$\mathcal{H}^{(2)} = \hbar I_z \frac{\omega_Q^2}{12\omega_0} \tag{36}$$

shifts the $m = \pm 1$ energy levels of a spin 1 by an equal amount in opposite directions. While this preserves the centre of gravity of the single-quantum doublet, it affects the double-quantum precession frequency in a manner which interferes with the measurement of the chemical shift. This effect becomes non-linear as the Larmor frequency decreases, as illustrated by Creel, von Meerwall and Barnes[21] who studied the ^{14}N frequencies as a function of B_0 (Fig. 17).

In the conventional single-quantum spectrum of nuclei with $I = 3/2$ such as ^{23}Na, only the central $(-1/2, +1/2)$ transition is usually observed because it is not broadened like the $(\pm 1/2, \pm 3/2)$ satellite transitions in the single-quantum spectrum. Since the double-quantum frequencies are also broadened by the quadrupole splitting, Vega and Naor[56] have explored the triple-quantum spectra of ^{23}Na in single crystals of sodium ammonium tartrate tetrahydrate. Selective triple-quantum pulses are inefficient in these systems $(\omega_1^3/\omega_Q^2 \ll 1)$ and it is necessary to employ modulated pulses for the excitation of the triple-quantum coherence. The latter's precession frequency provides insight into the orientation dependence of the second order quadrupole interaction. Since the triple-quantum experiment is most efficient when the modulation frequency matches the quadrupolar splitting in the single-quantum spectrum, the experiment is suitable for the indirect detection of the single-quantum satellites and represents an alternative to the scheme proposed by Polak and Vaughan.[57] In the presence of two inequivalent crystal sites with different quadrupole splittings, the modulation frequency can be chosen to select the triple-quantum spectrum of either site, as shown in Fig. 18.

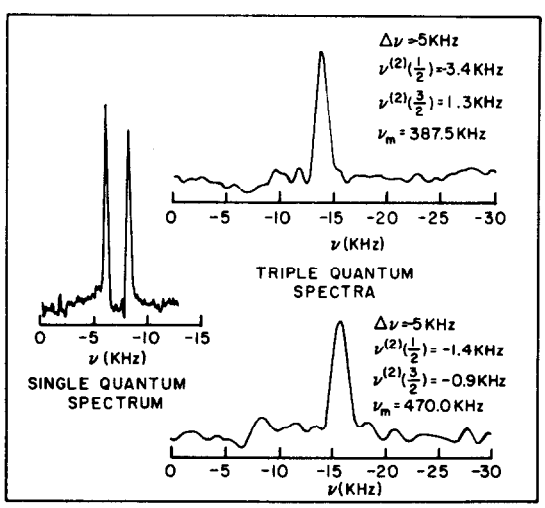

FIG. 18. Single- and triple-quantum spectra of ^{23}Na in an oriented single crystal of sodium ammonium tartrate tetrahydrate. The triple-quantum coherence of the two non-equivalent sites can be excited selectively by adjusting the modulation of the RF field to the quadrupolar splittings characteristic of the two sites. (Vega and Naor.[56])

6.2. *Scalar and Dipolar Coupled Systems*

The detailed structural information available from dipolar couplings has led to extensive NMR studies of molecules dissolved in partially oriented liquid crystals.[98–100] Aside from bond lengths and angles, it is possible to determine the quadrupole coupling constants and the anisotropy of various interactions. For all but the simplest systems, the proton spectra of oriented molecules tend to be quite complicated. For example, the conventional single-quantum spectrum of partially oriented benzene has some 76 transitions.[101] In principle, such spectra can be analysed by iterative procedures to yield the magnitudes and the relative signs of the various couplings (in the case of benzene, there are only three distinct dipolar and three scalar interactions). In practice however, the number of near-degenerate transitions may render the analysis quite difficult.

Multiple-quantum NMR has been applied in these cases to simplify the information content, because the number of possible transitions drops dramatically for higher-order multiple-quantum spectra. In a system of N non-equivalent spins 1/2, the number of possible p-quantum transitions is given by [91]

$$Z_p = \binom{2N}{N-p} \quad \text{for} \quad 1 \leqq p \leqq N \tag{37}$$

while the number of zero-quantum transitions is

$$Z_0 = \frac{1}{2}\left\{\binom{2N}{N} - 2^N\right\}. \tag{38}$$

The number of transitions is further reduced in systems with magnetic equivalence.[67,91] The tremendous simplification obtained for higher-quantum transitions has been demonstrated by Drobny *et al.*[48] in partially oriented benzene and 4-cyano-4′[$^2H_{11}$]pentyl-biphenyl, where coherences up to eighth order could be successfully excited. The simplification achieved in these spectra represents an alternative to isotopic substitution, which is the traditional, cumbersome cure for excessively complex proton spectra. The multiple-quantum spectra of oriented benzene in Fig. 19 shows essentially all possible transitions and illustrates the dramatic decrease in the number of lines as one progresses to the six-quantum transitions.[48] In this experiment, the coherences were excited by the broadband double-pulse technique discussed in Section 4.2. The lines can be significantly narrowed by refocussing the

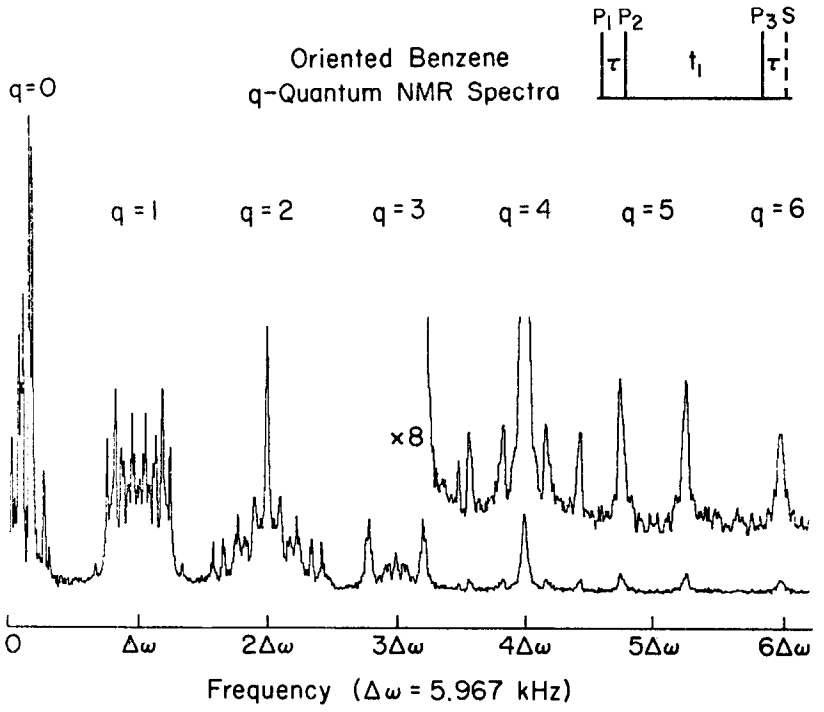

FIG. 19. Proton multiple-quantum spectrum of benzene oriented in a nematic solvent. The multiple-quantum coherences of all orders are excited by varying the interval in the 90°–τ–90° sequence. The lines are subject to increasing inhomogeneous broadening for high-order quantum transitions, but can be narrowed substantially by refocussing techniques. The simplicity of the 4-, 5- and 6-quantum spectra greatly aids the analysis. The magnitude spectra obtained for 11 τ-values spaced at 0.1 msec intervals from 9.6–10.7msec were added: the evolution period ranged from 0–13.8 msec in 13.5 μsec intervals for each value of τ. A single sample point was taken at a time τ after the monitoring pulse. (Drobny *et al.*[48])

inhomogeneous decay of the transverse coherence, a procedure which acquires increasing importance for high-order transitions (see Section 7). In principle, these spectra can be analysed much like ordinary high-resolution spectra to yield the magnitudes and the relative signs of the dipolar and scalar couplings, and the simplified assignment should facilitate the convergence of the iterative calculations.

In single-quantum NMR, it is usually not possible to assign the various resonances to an energy level diagram without some additional knowledge about the connectivity relationships, traditionally obtained from double resonance experiments.[102–5] As an alternative, the energy level diagram can be constructed with the aid of the zero-quantum spectrum in conjunction with the ordinary single-quantum spectrum.[91] A transition frequency ω_{rs} between two energy levels ψ_r and ψ_s with the same (unknown) quantum number m (e.g. the $\alpha\beta$ and $\beta\alpha$ states in a system of two coupled spins having $I = 1/2$) must be equal to the difference of two single-quantum frequencies $\omega_{rs} = \omega_{rt} - \omega_{st}$, ψ_t being an arbitrary state which differs from ψ_r and ψ_s by $\Delta m = \pm 1$. Since the number of possible states ψ_t is a single-valued function of m, the number of triangular relationships of the type $\omega_{rs} = \omega_{rt} - \omega_{st}$ identifies the quantum number m. In this manner, it is possible to assign the transitions to the energy level diagram,[67] although accidental degeneracies may introduce uncertainties in the assignment. A similar procedure is possible with the knowledge of double-quantum frequencies, as Anderson, Freeman and Reilly have demonstrated in the early days of CW multiple-quantum NMR.[4]

6.3. *Multiple-Quantum Tickling*

In more complex systems, the mere existence of triangular additivity relationships among the zero- and single-quantum transition frequencies may not

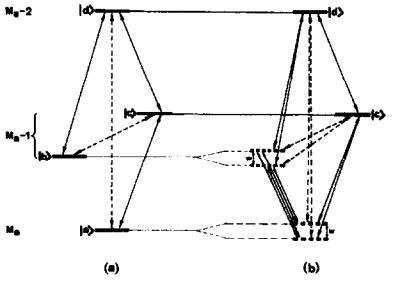

FIG. 20. Energy level diagram for two coupled spins-1/2 subjected to a continuous selective irradiation of the (a, b) transition. The time-dependent perturbation can be represented by splitting each of the levels a and b into a pair of virtual levels. All zero-, single- and double-quantum transitions which have an energy level in common with the irradiated transition split into doublets. (Wokaun and Ernst.[106])

be sufficient to identify the energy levels involved. The connectivities may be explored in a "spin-tickling" experiment,[105] which uses a selective irradiation of one transition (r,s) to impose a time-dependence on the states ψ_r and ψ_s to induce a splitting of all transitions connected with these states. This experiment has a direct analogue in multiple-quantum NMR, which has been discussed in detail by Wokaun and Ernst.[106] Two energy levels in a system of two coupled spins having $I = 1/2$, shown in Fig. 20, are modulated by the application of a continuous RF field at one of the allowed transitions. This can be represented heuristically by "virtual levels", shown in Fig. 20b, much like any modulation can be represented by sidebands.

It is clear from inspection of the figure that all transitions connected to the levels a and b will be split into doublets, regardless of whether or not they are single, zero or double-quantum transitions. In actual fact, this classification is no longer strictly meaningful, since the quantum number m is blurred by the mixing of the states. The multiple-quantum coherence may be excited by a $90°$–τ–$90°$ sequence and subjected to a continuous irradiation during the evolution period. As usual, a monitoring pulse is required to convert the invisible coherence into ordinary magnetization. Alternatively, it is possible to excite only single-quantum magnetization at the beginning of the t_1 period, and rely on the tickling field to create multiple-quantum coherence. In this manner, only those coherences that are connected with the irradiated transition are excited. It is a prerequisite for the observation of multiple-quantum tickling effects that the second frequency differ from the carrier frequency used for the pulses and the receiver reference.

6.4. *Multiple-Quantum Decoupling*

The theoretical development associated with multiple-quantum NMR, notably the introduction of single-transition operators,[42,69,70] has triggered a renewed interest in the mechanism of spin decoupling. The established way of calculating the spectrum of a spin S in the presence of a continuous, coherent RF field applied to a coupling partner I involves the diagonalization of the Hamiltonian in a frame where the decoupling field appears stationary.[107] This approach has been extended to ordered phases with dipolar and quadrupolar splittings.[108,109] The decoupling is most efficient when the frequency is exactly on resonance, forcing the I spins to be quantized in the transverse plane of the rotating frame, so that the scalar product I_zS_z vanishes. In all but the simplest systems, numerical calculations are necessary to predict the efficiency of the decoupling. To decouple deuterium nuclei in oriented systems, the decoupling field must compete not only with homo- and hetero-nuclear dipolar couplings, but also with the quadrupole interaction, which may be in excess of 100 kHz. Hewitt, Meiboom and Snyder[110] studied partially oriented deuterated systems and demonstrated that efficient decoupling is possible with RF fields that are much weaker than the quadrupole coupling, provided the decoupler is positioned precisely in the middle of the deuterium doublet. In this manner, the deuterium-decoupled spectrum of the residual protons in 82% deuterated cyclohexane could be obtained, representing an important simplification in comparison with fully protonated cyclohexane in oriented media.

Pines, Ruben, Vega and Mehring[111] showed that in the solid state it is possible to obtain a spectrum of the residual protons in deuterated polycrystalline ice without resorting to a prohibitive RF field strength B_2 to decouple the deuterium nuclei. The spectrum shown in Fig. 21 reveals a typical shift anisotropy powder pattern, which would be obscured by homonuclear dipolar interactions if the protons were not diluted.

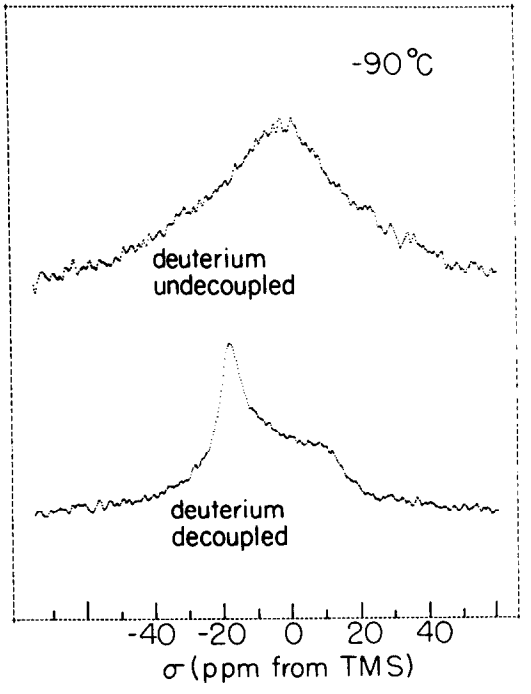

FIG. 21. Single-quantum spectra of the residual protons in deuterated polycrystalline ice. The powder pattern arising from the anisotropy of the proton chemical shift is clearly resolved in the presence of deuterium double-quantum decoupling. (Pines *et al.*[111])

The requirement that the deuterium decoupler should be positioned in the centre of the quadrupolar doublet is because the decoupling field acts like a selective double-quantum irradiation. Provided $\gamma B_2 \ll \omega_Q$, the double-quantum nutation occurs at an effective frequency $(\gamma B_2)^2/\omega_Q$ and the populations of the $m = \pm 1$ states are "stirred" continuously by the decoupler. The rapid drop in the decoupling efficiency observed if the irradiation frequency is moved away from exact resonance is also explained by the double-quantum nutation.[112,113] Finally, the

appearance of "tickling" satellites for weak irradiation can be accounted for by considering the effect of the RF field on the double-quantum transition alone.[109,110,113] For increasing field strength however, it becomes necessary to include the effect on the allowed transitions as well.[113]

6.5. *Selection of Multiplets*

Single-quantum proton spectra of large molecules in solution with homonuclear scalar couplings often present accidentally overlapping multiplets. In some cases, it may be possible to unravel the information by separating the scalar splittings and the chemical shift in orthogonal frequency domains by two-dimensional spectroscopy.[114] In many instances, it may be sufficient to simplify the spectrum by eliminating, for example, the singlets and retaining only the doublets. This can be achieved by transferring the doublet magnetization into double-quantum coherence, which can be retrieved selectively because of the characteristic response to RF phase shifts. The offset-independent excitation sequence 90°_x–τ–180°_x–τ–90°_x can be used to create double-quantum coherence simultaneously for most doublets, since vicinal proton–proton couplings are all of the same order of magnitude. Instead of allowing the double-quantum coherence to evolve, it is immediately transferred back into observable magnetization. By applying the phase-cycling schemes discussed in Section 5.3, it is possible to observe only that part of the magnetization which has been transferred back and forth between single- and double-quantum coherence.[115] The spectrum shown in Fig. 22 has been simplified in this manner by eliminating the singlets. Further delays can be used to restore the normal phases of the doublet components. This technique may find applications in proton spectroscopy of proteins and nucleotides.

Bax *et al.*[146] have developed a closely related technique for the observation of homo-nuclear carbon-13 couplings in natural abundance.

7. RELAXATION MEASUREMENTS

The information contained in the transverse relaxation of multiple-quantum coherence is often complementary to ordinary T_2 measurements. The dephasing of multiple-quantum coherence in inhomogeneous fields is more serious however than the T_2^* decay of ordinary magnetization, because a spatial variation of the resonance frequency $\Delta\omega = \gamma\Delta B_0(r)$ is amplified by a factor p

$$\sigma^p(t_1) = \sigma^p(o)\exp\{-ip\Delta\omega t_1\}. \qquad (39)$$

Clearly, zero-quantum coherences ($p = 0$) have the gratifying property that the transverse decay is completely insensitive to the field inhomogeneity.[47,91] Since zero-quantum transitions link states with the same quantum number m, the Zeeman splitting $\Delta m\gamma B_0$ does not affect the zero-quantum precession frequencies, which provide a direct measure of the scalar or dipolar couplings. Of course, the magnetic field should be sufficiently homogeneous to allow the detection of a well-resolved single-quantum spectrum after the monitoring pulse. This requirement limits the prospect of obtaining high-resolution spectra in arbitrarily inhomogeneous fields.

For multiple-quantum transitions with $p \geqq 2$, the use of refocussing techniques is often essential, except for a few favourable cases where the natural linewidth is significant compared to the inhomogeneous contribution.[91,116]

7.1. *Multiple-Quantum Echoes*

The refocussing of inhomogeneous dephasing of multiple-quantum coherence is closely analogous to the well-known echo experiments due to Hahn[117,118] and Carr and Purcell.[119] In systems where non-selective pulses can be applied, a simple 180° pulse at the mid-point of the evolution period will flip the multiple-quantum coherence into a symmetrical position in the rotating frame. This

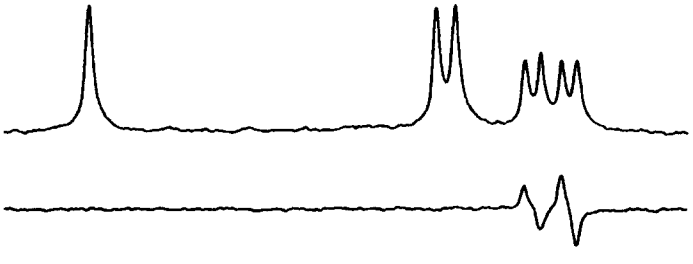

FIG. 22. The conventional single-quantum spectrum (top) of the aromatic protons of a mixture of nucleotides consists of a superposition of doublets (due to cytidine and uridine 5′ monophosphates) and singlets (due to adenosine and guanosine 5′ monophosphates). The doublets can be observed selectively by transferring the coherence back and forth between single- and double-quantum coherence, as shown in the lower spectrum. (Bodenhausen and Dobson[115].)

allows the fast isochromats to catch up with slow components, just like in ordinary spin echoes. The monitoring pulse is then applied to the multiple quantum coherence at the top of the echo. To counter the effects of diffusion, a train of 180° pulses can be applied in analogy to Carr and Purcell's method "B".[72,119]

Other systems, which cannot be covered adequately with non-selective pulses, may require special refocussing techniques. In ^{27}Al, a selective multiple quantum pulse may be applied half-way between the allowed transitions (a,b) and (b,c) (see Fig. 8) to flip the double-quantum coherence σ_{ac} through an angle $\omega_1^2\tau_p/\omega_Q = \pi$.[68] Alternatively, the σ_{ac} coherence may be converted into ordinary σ_{ab} magnetization, which is then refocussed by a 180° pulse and transferred back into σ_{ac} for the second half of the evolution period.[51,54]

According to Meiboom and Gill,[120] the phase of single-quantum echoes is inverted if the refocussing pulse is shifted in phase by 90°. Bodenhausen *et al.*[40] have shown that a p-quantum echo is inverted by a shift of $90°/p$ in the RF phase of the refocussing pulse (i.e. a 45° phase shift for a double-quantum echo). The phenomenological description discussed in Section 3.2 uses a d-orbital to represent a double-quantum coherence (Fig. 5). If a $d_{x^2-y^2}$ function is rotated by 180° about an RF field which bisects the x and y axes ($\phi = 45°$), the positive and negative lobes are interchanged and the function changes its sign. If on the other hand the 180° pulse is applied along either the x or y axis ($\phi = 0°$ or 90°), the d-orbital remains invariant, in agreement with double-quantum behaviour. These properties can be employed to distinguish the desired echo signal from a variety of non-ideal coherence transfer processes. The deuterium double-quantum echoes in Fig. 23b have been obtained with a refocussing pulse deliberately set to 90° instead of 180°. The amplitude anomalies, which arise from undesirable coherence transfer processes, are removed by a phase-cycling technique known as "hexcycle".[40] Such techniques acquire particular importance when the "hard" pulse approximation cannot be easily satisfied.

In systems with multiple-quantum transitions of various orders, the use of refocussing pulses removes the offset $p\Delta\omega$ which is responsible for spreading the various groups of signals in Fig. 19. To prevent the echoes of all orders p from "piling up" at $F_1 = 0$, an *artificial* chemical shift can be introduced by advancing the phase of the excitation in subsequent t_1-increments.[40,48,121] If these "time-proportional phase-increments"[48] are chosen to be $\Delta\phi = 180°/q$, a p-quantum echo appears displaced from $F_1 = 0$ by a fraction p/q of the F_1 spectral width.[40] As in single-quantum echoes, non-selective 180° pulses do not refocus quadrupolar or homonuclear scalar and dipolar splittings, and the echoes feature a multiplet structure reminiscent of J-spectroscopy.[122,123] The multiple-quantum spin echo spectrum of oriented benzene[48] is quite similar to the spectrum shown in Fig. 19, except for the linewidths which are much narrower for the higher-order transitions.

7.2. *Coherence Transfer Echoes and Stimulated Echoes*

If the inhomogeneous dephasing of multiple-quantum coherence is *not* refocussed, the amplitude of the magnetization detected after the monitoring pulse will be spatially inhomogeneous, reflecting a variation in the phase of the multiple quantum coherence. This may lead to "coherence transfer echoes" in the detection period, a phenomenon reported by the Kyoto group[51] and discussed in detail by Maudsley, Wokaun and Ernst.[124] While

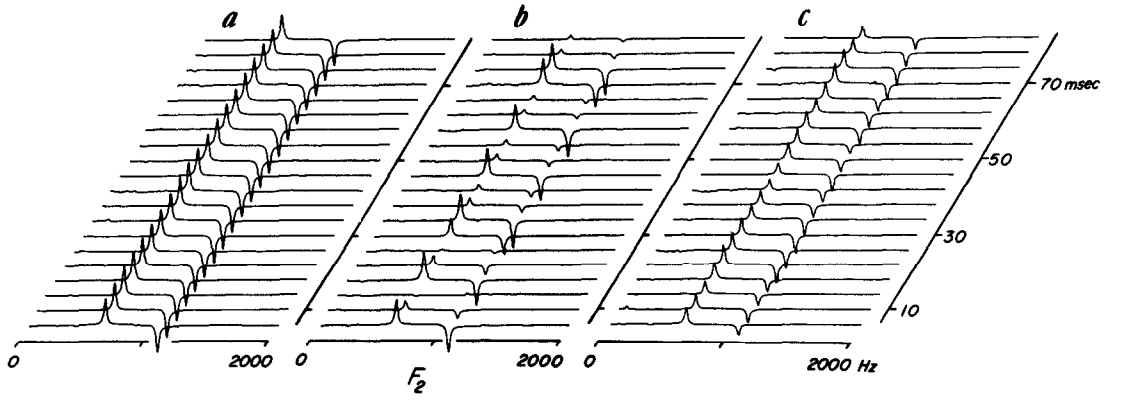

FIG. 23. Deuterium spectra of $CDCl_3$ partially oriented in polybenzylglutamate, obtained by a double-quantum spin-echo sequence 90°–τ–90°–$t_1/2$–α–$t_1/2$–90°-acquisition. In (*a*) the flip angle α was set to 180° and the absence of modulation indicates that the double-quantum precession has been refocussed properly. In (*b*), the refocussing pulse was purposely set to 90°, resulting in a variety of non-ideal coherence transfer processes. In (*c*), the 90° pulse was retained, but undesirable coherence transfers were eliminated by a 16-step phase-cycling sequence. The echoes are essentially ideal in spite of very adverse conditions. (Bodenhausen, Vold and Vold.[40])

the defocussing of the multiple quantum coherence is accelerated by the p-fold dependence on the field inhomogeneity, the refocussing occurs at the slower rate of single-quantum coherence. Hence the echo will appear asymmetrically in time at $t_2 = pt_1$[67,124] and the time constant of the echo decay reflects a combination of two transverse relaxation times. Coherence transfer echoes tend to distort the two-dimensional lineshapes, although the decay rate can in principle be retrieved from a skew cross-section.[47,124] Coherence transfer echoes are of course avoided altogether if a refocussing pulse is used in the evolution period.

Like other experiments involving more than two pulses, multiple-quantum experiments can lead to stimulated echoes if the spatial variation of the phase is stored in the diagonal elements of the density matrix. Such effects have been reported by Hatanaka and Hashi[68] in ^{27}Al and by Wokaun[67] in scalar-coupled systems.

7.3. *Rotary Echoes and Spin-Locking*

If a multiple-quantum coherence is forced to nutate around a continuous RF field,[43,44] a damped sinusoidal behaviour is observed, similar to Torrey oscillations in single-quantum NMR.[125] Since the nutation frequency of p-quantum coherence is proportional to ω_1^p, RF inhomogeneity may lead to a rapid damping of the signals. This problem can be alleviated by a double-quantum analogue of Solomon's rotary echo.[126] While the sense of the nutation of ordinary magnetization is reversed by a 180° phase shift, the double quantum nutation requires a 90° phase shift.[43,44] The formation of a rotary echo in ^{27}Al is shown in Fig. 24, where the inhomogeneous RF field causes a rapid dephasing which can be counteracted by a 90° phase-shift.

The information contained in this kind of experiment should be analogous to the Torrey experiment, where the decay is determined by an average of the longitudinal and transverse relaxation rates.[125]

Just as in single-quantum NMR, it is possible to apply the idea of spin-locking[127,128] to multiple-quantum NMR.[44,129] The RF field is applied half-way between the allowed transitions to affect the double-quantum transition selectively, and after a 90° pulse, the RF phase is shifted by 45° to achieve the spin-locking effect. The $T_{1\rho}$ decay constant is sensitive to relaxation mechanisms with spectral components in the audio frequency range. This can be verified in ^{27}Al by introducing a modulation of the B_0 field. The spin-locking of the double-quantum coherence is perturbed when the modulation matches the nutation frequency,[129] in a manner reminiscent of rotary saturation experiments.[130]

A more recent study by Hatanaka and Hashi[131] employs the simultaneous irradiation of the two allowed transitions (a, b) and (b, c) in ^{27}Al (see Fig. 8). The transverse magnetization is periodically shuffled among σ_{ab}, σ_{bc} and σ_{ac}. To counteract the RF inhomogeneity, a phase-reversal is required which leads to coherence transfer *rotary* echoes.[131] These should not be confused with the coherence transfer echoes discussed by Maudsley *et al.*[124] The time constant of the rotary echo decay is much longer than the T_2 of either single- or double-quantum coherence, a phenomenon ascribed to the quenching of the dipolar interaction. These experiments may provide new insight into the mechanism of dipolar relaxation.[132]

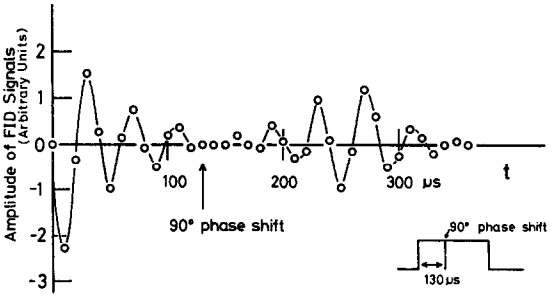

FIG. 24. The double-quantum coherence in ^{27}Al, nutating about a continuous RF field applied half-way between two single-quantum transitions, gradually dephases because of the RF inhomogeneity. A 90° phase-shift reverses the sense of the nutation and leads to a rotary echo of the double-quantum coherence. (Hatanaka, Ozawa and Hashi.[43])

8. MOTIONAL STUDIES

The strength of multiple-quantum NMR lies in its ability to select an arbitrary pair of eigenstates ψ_r and ψ_s, without regard to a selection rule, and to measure the transverse decay of an arbitrary coherence σ_{rs}. The mathematical description of transverse relaxation is essentially the same for multiple- and single-quantum transitions. Provided none of the precession frequencies is degenerate, the coherence decays exponentially:

$$|\sigma_{rs}(t_1)| = |\sigma_{rs}(o)| \exp\{-R_2(r,s)t_1\}. \qquad (40)$$

The relaxation rate $R_2(r,s) = 1/T_2(r,s)$ can be evaluated with the Redfield equation[35,133] which is directly applicable to multiple-quantum relaxation:

$$R_2(r,s) = -R_{rsrs} = \frac{1}{2\hbar}\left[-2J_{rrss}(o) + \sum_t J_{trtr}(\omega_{tr}) + \sum_t J_{tsts}(\omega_{ts})\right] \qquad (41)$$

This equation can be recast in an equivalent form which highlights the contributions of two different mechanisms:

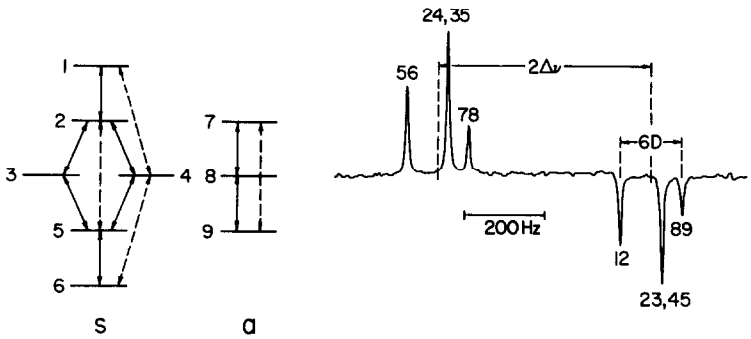

FIG. 25. The energy level diagram of a system of two dipolar coupled equivalent deuterons consists of 6 symmetrical and 3 anti-symmetrical states. The corresponding transitions are well separated in the single-quantum spectrum of CD_2Cl_2 in a nematic solvent (right). The spectrum is aliased about the carrier frequency; the actual separation between the triplets is *ca.* 15 kHz. Four double-quantum transitions, indicated by dotted lines in the energy-level diagram, are independent of the quadrupolar interaction and provide useful relaxation information. (Vold, Vold, Poupko and Bodenhausen.[72])

$$R_2(r,s) = \frac{1}{2}\left[\sum_{t\neq r} W_{tr} + \sum_{t\neq s} W_{ts}\right] + \frac{1}{2\hbar} \times \int_{-\infty}^{+\infty} \overline{\{(r/\mathscr{H}(t)/r) - (s/\mathscr{H}(t)/s)\}} \times \overline{\{(r/\mathscr{H}(t+\tau)/r) - (s/\mathscr{H}(t+\tau)/s)\}}\, d\tau \quad (42)$$

$$R_1 = \frac{3\pi^2}{2}\left(\frac{e^2qQ}{h}\right)^2 \{J_1(\omega_0) + 4J_2(2\omega_0)\} \quad (43)$$

$$R_2(+1,-1) = \frac{3\pi^2}{2}\left(\frac{e^2qQ}{h}\right)^2 \times \{J_1(\omega_0) + 2J_2(2\omega_0)\}. \quad (44)$$

The first term represents non-adiabatic contributions to the linewidth which originate from the finite lifetimes imposed by the spin–lattice relaxation. The second term in equation (42) is the adiabatic contribution, which reflects the fluctuations of the energy levels of the states ψ_r and ψ_s. It is clear that *concerted* fluctuations, which shift the energy of both states in the same direction by the same amount, do not contribute to the adiabatic relaxation. Multiple-quantum relaxation may therefore be insensitive to certain mechanisms. On the other hand, some processes may cause energy fluctuations that affect the states ψ_r and ψ_s simultaneously in *opposite* directions. In this case, multiple quantum relaxation may contain more information than conventional T_2 measurements. The following two sections provide an example of each case.

8.1. *Quadrupolar Relaxation*

Deuterium NMR is an attractive probe for motional studies, because the relaxation is determined only by the quadrupolar interaction, which is entirely intramolecular in origin. The motional spectrum of a single oriented deuteron can be described by a spectral density function $J(\omega)$, which has a different effect on the spin-lattice relaxation and the transverse double-quantum relaxation:[40,116,134]

This simple set of linear equations can readily be solved to determine $J_1(\omega_0)$ and $J_2(2\omega_0)$.[116] It is worth noting that the transverse decay of the double-quantum coherence is slower than the longitudinal relaxation. These equations do not include the effects of chemical exchange, which may be of importance in some exotic liquid crystalline solutions (such as $CDCl_3$ in polybenzylglutamate). Chemical exchange tends to hasten the dephasing of double-quantum coherence.[40]

In the particular case of a single oriented deuteron (such as $CDCl_3$ and DCCCN in nematic solvents) the determination of $J_1(\omega_0)$ and $J_2(2\omega_0)$ from equations (43) and (44) can be cross-checked by selective T_1 experiments.[134] Both methods turn out to be remarkably consistent, indicating that multiple-quantum decay rates can indeed be used as a reliable source of information.[116]

In saturated hydrocarbon chains, the selective deuteration of one methylene group is a powerful technique for motional studies, as shown by Hsi *et al.* for liquid crystals.[92] The relaxation of an oriented CD_2 moiety has been described in detail by Vold and co-workers,[71] who in their experimental illustration used the model system of CD_2Cl_2, partially oriented in a nematic solvent. Like in hydrocarbon chains, the rotational diffusion in the CD_2 plane is preferred strongly, but in contrast to hydrocarbons, there is no need to decouple the residual protons. This greatly simplifies the experimental problems in these highly temperature-dependent systems. The energy level

diagram appropriate for a pair of partially oriented, coupled deuterons is shown in Fig. 25, together with the single-quantum spectrum of CD_2Cl_2 in a nematic solvent.

To describe the motion of a CD_2 group in a satisfactory manner, it is necessary to define two spectral density functions, one for the autocorrelation of the reorientation of a C–D bond, the other for the cross-correlation of the motion of the two deuterons:[71]

$$J_q^A(\omega) = \int_0^\infty F_q(t)F_q^*(t-\tau)\exp(-i\omega\tau)\,d\tau \quad (45)$$

$$J_q^C(\omega) = \int_0^\infty F_q(t)E_q^*(t-\tau)\exp(-i\omega\tau)\,d\tau \quad (46)$$

where $F_q(t)$ and $E_q(t)$ are spherical harmonics of rank q describing the orientation of the first and the second C–D bond, assumed to be parallel to the principal field gradient axis. The average values, which do not vanish in an anisotropic medium, must be subtracted from these functions. It turns out that six independent values of the spectral density functions must be determined, which are listed in Table 2. If one does not wish to make any assumptions about the dependence of the spectral density functions on the Larmor frequency, at least six independent measurements are necessary to determine the six parameters. This requires a sophisticated weaponry, including selective inversion recovery experiments and T_2-measurements of both single- and multiple-quantum coherence.

Although the energy-level diagram indicates a total of 18 possible coherences, only 7 independent transverse relaxation rates can be measured in practice. Their dependence on the spectral density functions is shown in Table 2, which in effect represents an overdetermined system of linear equations.

Some of the double-quantum coherences precess at the same frequency and give rise to non-exponential relaxation, but the two-dimensional lineshapes can nevertheless be analysed in terms of spectral densities.[72] A typical double-quantum spectrum of oriented CD_2Cl_2 is shown in Fig. 26, where the F_1 linewidths provide a measure of the transverse double-quantum relaxation.

Numerical determination of the cross-correlation terms reveals that the cross- and auto-correlation functions are similar in magnitude (Table 2, bottom line). The dependence on the Larmor frequency reveals contributions to $J_1^A(\omega_0)$ which are probably due to slow hydrodynamic fluctuations of the order director of the liquid crystalline solvent.

8.2. *Correlated Random Fields*

Selective deuteration often presents synthetic difficulties, and it may be desirable to turn to coupled

TABLE 2. Relaxation of an oriented CD_2 system in terms of spectral densities of motion

	$J_0^A(0)$	$J_1^A(\omega_0)$	$J_2^A(2\omega_0)$	$J_0^C(0)$	$J_1^C(\omega_0)$	$J_2^C(2\omega_0)$
Single-Quantum Transverse Relaxation						
$R_2(1,2)$	$3C/2$	$5C/2$	$3C$	0	C	0
$R_2(2,4)$*	$3C/2$	$5C/2$	$3C$	0	C	$2C$
$R_2(7,8)$	$3C/2$	$5C/2$	$3C$	0	$-C$	$-2C$
Double-Quantum Transverse Relaxation						
$R_2(1,4)$	0	$2C$	$4C$	0	0	$2C$
$R_2(2,5)$*	$3C/2$	$3C$	$2C$	$-3C/2$	$2C$	0
$R_2(7,9)$*	$3C/2$	$3C$	$2C$	$-3C/2$	$-2C$	0
Quadruple Quantum Transverse Relaxation						
$R_2(1,6)$	0	$2C$	$4C$	0	0	0
Longitudinal Relaxation						
R_1 (non-selective)	0	C	$4C$	0	0	0
R_1 (selective)	0	$5C/2$	C	0	0	0
R_1 (selective)	0	$4C$	$-2C$	0	0	0
Numerical Results [psec]	3.7	3.6	1.4	3.7	1.9	0.9

The constant is defined as $C = \frac{3\pi^2}{2}\left(\frac{e^2qQ}{h}\right)^2$.

The terms marked with (*) are subject to cross-relaxation.

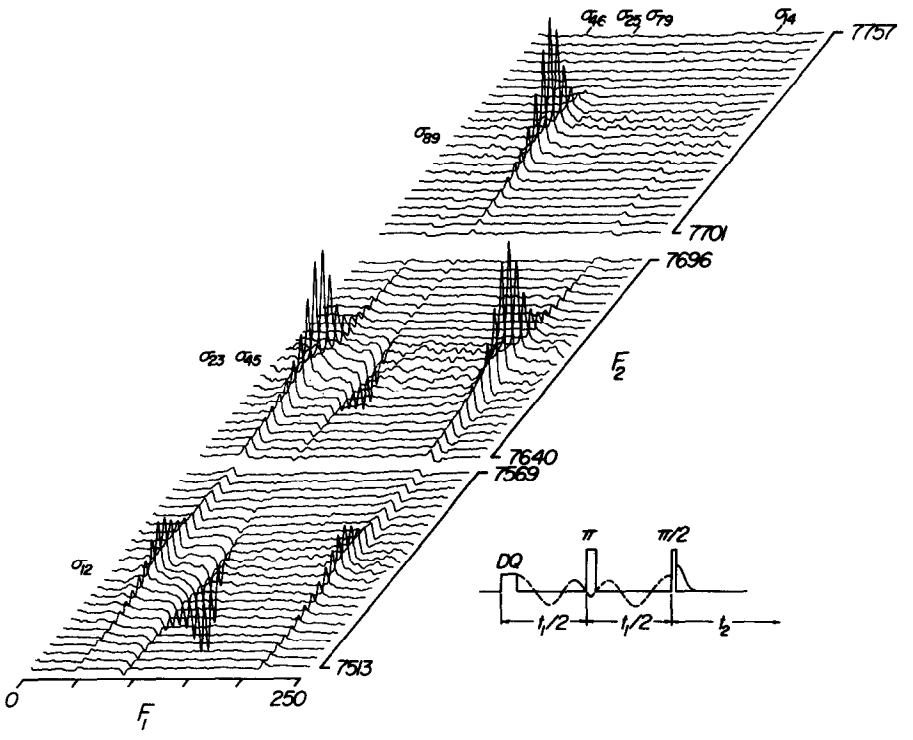

FIG. 26. The double-quantum signals of oriented CD_2Cl_2 appearing in the F_1-domain are spread in the single-quantum F_2 dimension to separate signals of different symmetry. The inhomogeneous dephasing is refocussed and the F_1-linewidths provide an accurate measure of the transverse relaxation of the various multiple-quantum coherences. The indices of the coherence terms σ_{pq} refer to the energy-level diagram in Fig. 25. Reproduced from reference 72.

protons or carbon–proton systems to investigate the molecular motion. The relaxation is usually more complicated and may involve intermolecular interactions, but the information can give a detailed picture of randomly fluctuating fields.

Consider a system of two weakly-coupled protons A and B, exposed to external fluctuating fields $B_{AZ}(t)$ and $B_{BZ}(t)$, which are assumed to be parallel to the static field B_0. This assumption leads to a simple Hamiltonian:[60,136]

$$\mathscr{H}(t) = -\gamma I_{AZ} B_{AZ}(t) - \gamma I_{BZ} B_{BZ}(t). \qquad (47)$$

The B-spin transition between the states

$$\psi_1 = |-1/2, -1/2\rangle \quad \text{and} \quad \psi_2 = |-1/2, +1/2\rangle$$

conserves the polarization of the A-spin. As a result, the adiabatic contribution to the transverse relaxation of the (1, 2) transition depends only on the field $B_{BZ}(t)$:

$$\{(1|\mathscr{H}(t)|1) - (2|\mathscr{H}(t)|2)\} = \gamma B_{BZ}(t). \qquad (48)$$

The transverse relaxation rate expressed in equation (42) is simply

$$R_2(1,2) = \frac{\gamma^2}{2\hbar} \int_{-\infty}^{+\infty} \overline{B_{BZ}(t) B_{BZ}(t+\tau)}\, d\tau + \text{non-adiabatic terms.} \qquad (49)$$

Assuming an exponential correlation function[91,136]

$$\overline{B_{BZ}(t) B_{BZ}(t+\tau)} = \overline{B_{BZ}^2} \exp(-\tau/\tau_c); \qquad (50)$$

equation (49) reduces to

$$R_2(1,2) = \frac{\gamma^2}{\hbar} \overline{B_{BZ}^2}\, \tau_c + \text{non-adiabatic terms.} \qquad (51)$$

A more thorough analysis includes the transverse components of the fluctuating fields, and the non-adiabatic contribution to the linewidth of a B-spin transition also depends on the spin-lattice relaxation of spin A. The resulting transverse relaxation rates are shown in Table 3. Neither the single-quantum linewidth nor the spin lattice relaxation of the weakly-coupled AB system give any information about the correlation of the fluctuating fields $B_A(t)$ and $B_B(t)$. To retrieve this information in weakly coupled systems, it is necessary to turn to zero- and double-quantum relaxation.[60,91] The adiabatic contri-

TABLE 3. Relaxation of two non-equivalent protons by partially correlated random fields

Single-Quantum Relaxation
$R_2(1,2) = R_2(3,4) = \gamma^2\tau_c\left[\overline{B_{AX}^2} + \overline{B_{BX}^2} + \overline{B_{BZ}^2}\right]$
$R_2(1,3) = R_2(2,4) = \gamma^2\tau_c\left[\overline{B_{AX}^2} + \overline{B_{BX}^2} + \overline{B_{AZ}^2}\right]$
Double-Quantum Relaxation
$R_2(1,4) = \gamma^2\tau_c\left[\overline{B_{AX}^2} + \overline{B_{BX}^2} + \overline{B_{AZ}^2} + \overline{B_{BZ}^2} + 2C_{AB}\sqrt{\overline{B_{AZ}^2}\,\overline{B_{BZ}^2}}\right]$
Zero-Quantum Relaxation
$R_2(2,3) = \gamma^2\tau_c\left[\overline{B_{AX}^2} + \overline{B_{BX}^2} + \overline{B_{AZ}^2} + \overline{B_{BZ}^2} - 2C_{AB}\sqrt{\overline{B_{AZ}^2}\,\overline{B_{BZ}^2}}\right]$

bution to the double-quantum relaxation is determined by

$$\{(1|\mathscr{H}(t)|1)-(4|\mathscr{H}(t)|4)\} = \gamma B_{AZ}(t)+\gamma B_{BZ}(t). \quad (52)$$

The transverse decay of the σ_{14} coherence is described by equation (42):

$$R_2(1,4) = \frac{\gamma^2}{2\hbar} \times \int_{-\infty}^{\infty} \overline{\{B_{AZ}(t)+B_{BZ}(t)\}\{B_{AZ}(t+\tau)+B_{BZ}(t+\tau)\}}\, d\tau + \text{non-adiabatic terms.} \quad (53)$$

The product leads to cross-terms which require an additional correlation function:[91,136]

$$\overline{B_{AZ}(t)B_{BZ}(t+\tau)} = C_{AB}\sqrt{\overline{B_{AZ}^2}\,\overline{B_{BZ}^2}}. \quad (54)$$

The coefficient C_{AB} varies between zero for totally independent fluctuations and unity for completely correlated fluctuating fields. Armed with this definition, one can reduce equation (53) to:

$$R_2(1,4) = \frac{\gamma^2}{\hbar}\tau_c\left[\overline{B_{AZ}^2}+\overline{B_{BZ}^2}+2C_{AB}\sqrt{\overline{B_{AZ}^2}\,\overline{B_{BZ}^2}}\right] + \text{non-adiabatic terms.} \quad (55)$$

A more comprehensive treatment includes the transverse components of fluctuating fields and yields the double- and zero-quantum relaxation rates given in Table 3. To provide an experimental verification of this theory, Wokaun and Ernst studied the relaxation

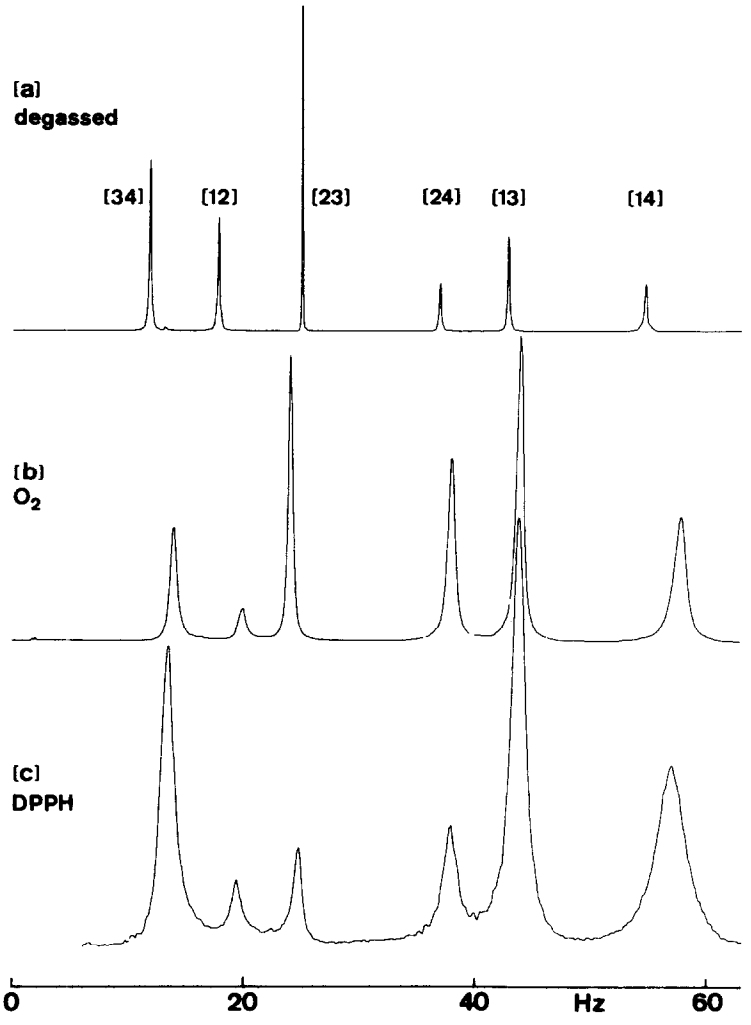

FIG. 27. Multiple-quantum spectra of the two coupled protons in 2,3-dibromothiophene, obtained by projecting a two-dimensional spectrum onto the F_1-axis. The linewidths of the zero-quantum transition (2,3) and the double-quantum transition (1,4) provide a measure of the correlation of the random field fluctuations induced by oxygen (middle) and 1,1-diphenyl-2-picryl-hydrazyl (below). Inhomogeneous broadening is accounted for by subtracting the linewidths of a degassed sample (top). (Wokaun and Ernst[91].)

induced by paramagnetic molecules in solution.[91] Although the relaxation is actually dipolar in origin, an adequate picture of the proton relaxation is obtained by considering the fluctuating magnetic fields induced at the sites of the protons A and B. By selecting paramagnetic molecules of different sizes, such as oxygen and 1,1-diphenyl-2-picryl-hydrazyl (DPPH), one can obtain different degrees of correlation of the random fields. This is because large paramagnetic molecules can only approach both protons simultaneously, while the smaller oxygen molecule can interact selectively with one of the protons. The effects on the zero- and double-quantum linewidths of the AB system are shown in Fig. 27.

The DPPH molecule leads to a correlation coefficient $C_{AB} = 0.89$, while oxygen induces less correlated fluctuations ($C_{AB} = 0.79$).

Different avenues have been explored by Tang and Pines,[137] who considered the effect of paramagnetic relaxation on the protons of a rapidly rotating methyl group. Unless the paramagnetic centre is precisely aligned with the C_{3V} axis, the symmetry is broken, and relaxation pathways which connect irreducible representations of the symmetry group become allowed.

The transverse relaxation of three independent single-, double- and triple-quantum coherences can be expressed by linear combinations of four spectral densities, which in turn are defined as admixtures of cross- and auto-correlation functions. This admixture is determined by a correlation parameter ξ which is equal to unity when the relaxation conserves the C_{3V} symmetry, and drops to zero when each proton is relaxed independently. To test this theory, the multiple-quantum linewidths of CH_3CN in a nematic solvent were measured in the presence of di-t-butylnitroxide radicals.[137] The concentration dependence (Fig. 28) indicates that the correlation parameter ξ is equal to unity, which is consistent with a picture where the time-scale of the methyl group rotation is much shorter than the lifetime of the interaction between the protons and the paramagnetic molecule.

Unlike the work of Wokaun and Ernst,[91] which relied on a simple subtraction to compensate for the T_2^* broadening, Tang and Pines[137] used multiple-quantum spin echoes in conjunction with time-proportional phase increments to measure the transverse relaxation.

9. MULTIPLE-QUANTUM INTERFERENCE

Many research workers involved in multiple-quantum NMR tend to agree that the experiments are surprisingly easy. Although optimizing the excitation may present a challenge, virtually any pulse sequence is capable of generating at least some accidental multiple-quantum coherence. It is not surprising therefore that some of the most treasured NMR methods turn out to be affected by multiple-

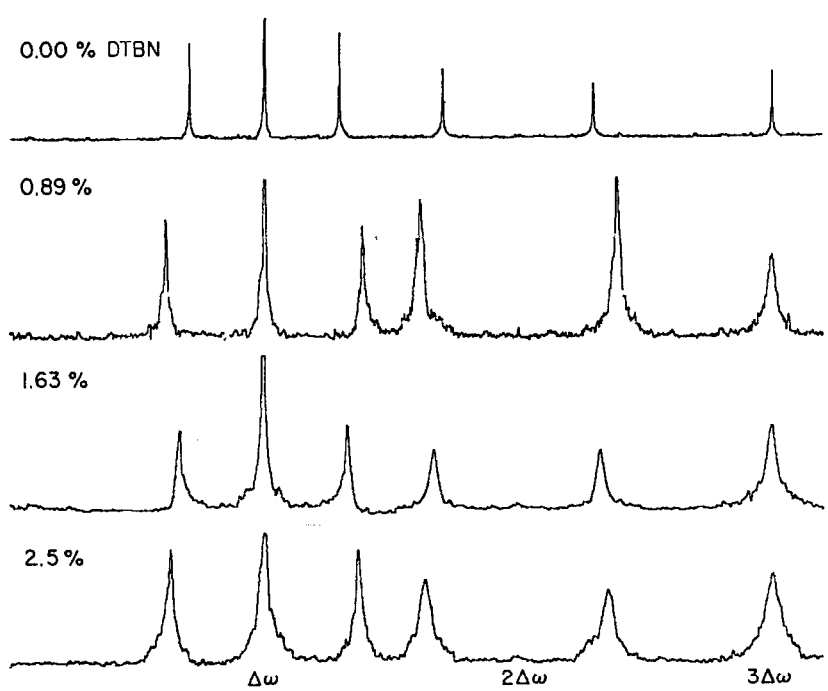

FIG. 28. Multiple-quantum spin-echo spectra of acetonitrile (CH_3CN) oriented in a nematic solvent. From left to right, the spectra show a single-quantum triplet, a double-quantum doublet and a triple-quantum singlet. The linewidths are linearly proportional to the concentration of di-t-butylnitroxide radicals. These experiments indicate that the symmetry of the CH_3 group is not broken by the relaxation process. Inhomogeneous broadening is removed by refocussing. (Tang and Pines[137].)

quantum phenomena, often quite contrary to the experimentalist's desire.

An example is the ubiquitous 180°–t–90° inversion recovery experiment[138] which normally employs strong, non-selective pulses. In actual practice, the "180°" pulse rarely brings about an ideal population inversion, and often generates spurious transverse magnetization, which is normally cancelled either by field gradient pulses[138] or by alternating the RF phase of the initial pulse.[139] If the RF power is limited and comparable in magnitude to the chemical shift difference or quadrupolar splitting in the spectrum, the population inversion pulse may unexpectedly acquire the character of a selective multiple-quantum pulse of the type discussed in Section 4.7. The 90° pulse, instead of merely sampling the population distribution, can also act as monitoring pulse and transfer multiple-quantum coherence into observable magnetization, thus perturbing the relaxation measurements. This problem is particularly severe in deuterium spectra of partially oriented samples, where the quadrupole splitting can easily exceed the strength of the RF pulses. Multiple-quantum interference leads to gross distortions of the inversion-recovery spectra, as shown in Fig. 29. Since the phase of the double-quantum coherence is invariant under a 180° RF phase shift, the usual phase-alternation schemes are ineffective. Fortunately, the sign of the double-quantum coherence may be reversed by advancing the RF phase of the initial pulse through 90°, a property which has been combined by Vold *et al.* with the traditional phase alternation into a four- or eight-step cycle,[140] which effectively cancels most multiple-quantum interference phenomena as can be seen in Fig. 29B. It should be noted that the oscillatory behaviour of the multiple-quantum interference depends on the offset $\Delta\omega$, and the misleading contributions to the signal might not be evident if the transmitter were positioned exactly on resonance.

A similar problem arises in solid-state relaxation measurements, where the Jeener–Broekaert experi-

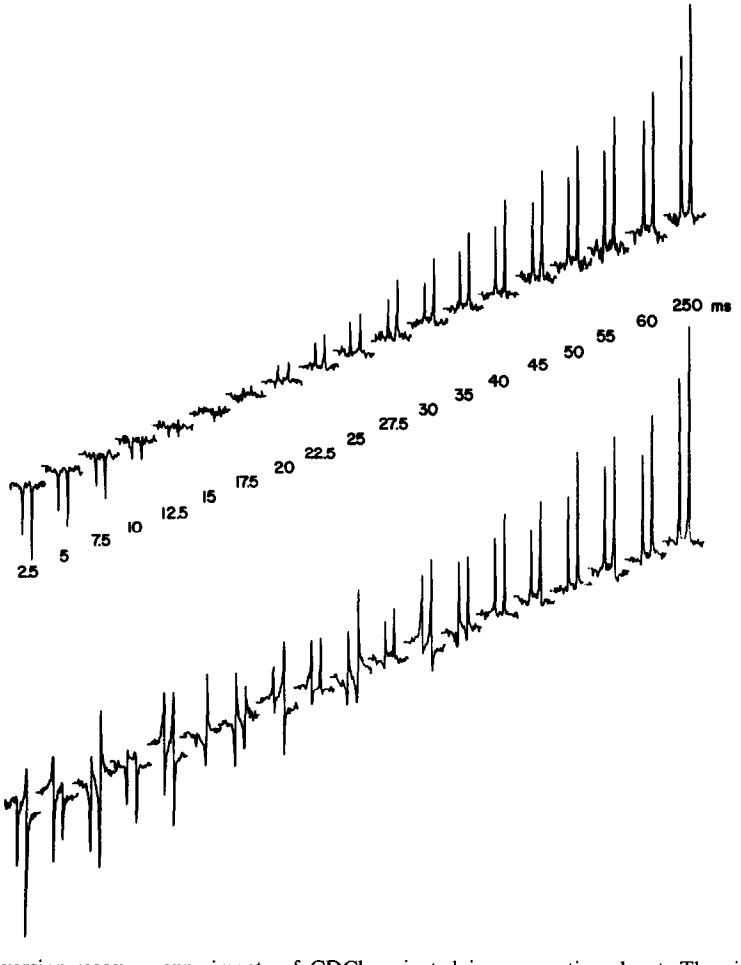

FIG. 29. Inversion-recovery experiments of $CDCl_3$ oriented in a nematic solvent. The signals of the quadrupolar deuterium doublet are aliased about the receiver frequency; the actual separation of the two lines is ca 30 kHz. The initial "180°" pulse generates spurious double-quantum coherence which is converted into observable magnetization by the 90° pulse. The interference cannot be suppressed by simple phase alteration (below) but phase-shifting through 90° cancels the double-quantum effects (top). (Vold and Bodenhausen[140].)

ment[141] uses a $90°-\tau-45°$ sequence to prepare a non-equilibrium state of dipolar order. The return to the thermal equilibrium is monitored by applying a 45° pulse at a time t_1 after the preparation. A recent study by Emid *et al.*[142] reveals that the preparation sequence tends to generate spurious multiple-quantum coherence, as evidenced by the modulation of the signals as a function of t_1.

A re-examination by Müller and Ernst[143] of the cross-polarization experiment proposed by Hartmann and Hahn[73] indicates that multiple-quantum coherence is involved in the course of the transfer process.

In two-dimensional experiments designed to study the time evolution of allowed single-quantum magnetization, continuous RF fields may be employed to decouple some of the interactions in the evolution period.[144] Wokaun and Ernst[106] have shown that multiple-quantum coherence may be generated if a system with transverse single-quantum magnetization is subjected to continuous irradiation. This can only occur, however, if the frequency of the second RF field differs from the carrier frequency used for the pulses, and Nagayama[144] avoided these complications by using the same frequency for both irradiations.

Generally, it is advisable to examine the exact state of a spin system just before an observation pulse is applied, paying special attention to non-vanishing density matrix elements belonging to forbidden transitions. Their contributions to the signal can easily be identified on the basis of the characteristic phase properties.

10. INSTRUMENTAL REQUIREMENTS

Like other forms of two-dimensional spectroscopy, multiple-quantum NMR requires reasonable long-term stability of the instrument. Since the evolution of the multiple-quantum coherence is mapped out point by point, the compilation of the t_1 domain "interferogram" often requires an overnight experiment.

In nematic liquid crystalline solutions, small temperature variations may have dramatic effects on the order parameter and hence on the quadrupolar splittings of deuterium spectra. In the systems studied by Vold and co-workers,[72] the frequency can vary by as much as 250 Hz per degree (for linewidths of the order of 10 Hz), requiring excellent temperature stability which in their laboratory could be achieved with a home-built control system.[135] Remaining frequency drifts in the F_2 domain can be compensated by shifting the $S(t_1, F_2)$ spectra individually prior to the Fourier transformation with respect to t_1. Alternatively, it is possible to integrate over an F_2-window wide enough to contain the wandering peaks. Failure to take such precautions results in severe lineshape distortions in the two-dimensional spectra.

The pioneering experiments on selective detection by Wokaun and Ernst[45] were carried out without actual phase shifts, by using a $270°_x$ pulse as an approximation to a $90°_{-x}$ pulse. However, the characteristic phase properties of multiple-quantum coherence can only be fully explored with a flexible device for the control of the RF phase. It is possible to incorporate a computer controlled switchable delay line, which can be obtained commercially. An alternative scheme, developed in the San Diego laboratory, is based on the digital division of a square wave signal and generates phase-shifts by deliberately missing a count in the division process.[145] This type of device is readily programmable and quite accurate since it operates in the time domain. Whether digital or analogue, the device should be capable of phase increments $\Delta\phi$ appropriate to the spin physics envisaged. In general, the higher the order p of the coherence that one wishes to observe selectively, the smaller $\Delta\phi$ should be. In multiple-quantum spin–echo spectroscopy, the phase-cycling shown in Fig. 23 requires increments $\Delta\phi = 90°/p$ for the selective observation of p-quantum echoes.

Some of the experiments require pulses at the same frequency but with different power levels. One can either use two different attenuators controlled by separate gating, or, alternatively, insert a computer-controlled RF attenuator in the transmitter system.[72]

The combination of multiple-quantum NMR with double resonance[106] requires two RF carriers which should have a defined phase relationship at the beginning of the evolution period. In practice, it is easy to generate the difference frequency in a double-balanced mixer and to use a zero-crossing point of this signal to trigger the RF pulse which initiates the experiment.[106]

Finally, multiple-quantum spectroscopy may be greatly simplified with a flexible pulse programmer and a convenient data handling system with disk storage. Much of the work reported in this review however has been carried out with relatively unsophisticated spectrometers primarily designed for conventional Fourier transform NMR.

11. CONCLUSIONS

At the time of writing, multiple-quantum NMR has undergone a tremendous renewal because of the introduction of pulsed excitation and indirect detection of the invisible coherence in the manner of two-dimensional spectroscopy. The techniques have clearly passed the stage of infancy, and a number of promising applications, particularly with regard to the simplification of spectral information and the analysis of molecular motion, all seem to indicate that multiple-quantum NMR has found a place among the established NMR methods. It is our belief that the spectrum of applications will continue to expand, both in dynamic as well as in static studies, not least

because, as Ernst put it once, the NMR spectroscopist will find it difficult to resist the temptation of the forbidden fruits of spectroscopy.

Acknowledgements—It is a pleasure to acknowledge the cooperation received in preparing this review from Drs. T. Hashi, R. R. Ernst, A. Pines, R. R. and R. L. Vold, S. Vega, S. Emid, M. Mehring, K. Packer, R. Freeman, R. Creel, D. Dubbers, L. Müller and Z. Luz, some of whom kindly provided manuscripts prior to publication, and many of whom gave their permission to reproduce figures. The contributions of M. Munowitz, who made innumerable constructive comments, are greatly appreciated. This work was supported by grant RR00995 from the Division of Research Resources of the National Institutes of Health and by the National Science Foundation through contract C-670.

REFERENCES

1. W. A. Anderson, *Phys. Rev.* **104**, 850 (1956).
2. J. I. Kaplan and S. Meiboom, *Phys. Rev.* **106**, 499 (1957).
3. S. Yatsiv, *Phys. Rev.* **113**, 1522 (1959).
4. W. A. Anderson, R. Freeman and C. A. Reilly, *J. Chem. Phys.* **39**, 1518 (1963).
5. K. A. McLauchlan and D. H. Whiffen, *Proc. Chem. Soc.* 144 (1962).
6. A. D. Cohen and K. A. McLauchlan, *Disc. Faraday Soc.* **34**, 132 (1962).
7. A. D. Cohen and D. H. Whiffen, *Mol. Phys.* **7**, 449 (1964).
8. J. I. Musher, *J. Chem. Phys.* **40**, 983 (1964).
9. M. L. Martin, G. J. Martin and R. Couffignol, *J. Chem. Phys.* **49**, 1985 (1968).
10. K. M. Worvill, *J. Magn. Reson.* **18**, 217 (1975).
11. R. A. Hoffman, *Adv. Magn. Reson.* **4**, p. 88, J. S. Waugh (ed.), Academic Press, New York (1970).
12. B. Gestblom, O. Hartmann and A. Bugge, *J. Magn. Reson.* **2**, 186 (1970).
13. B. Gestblom, *J. Magn. Reson.* **3**, 293 (1970).
14. F. Bloch and A. Siegert, *Phys. Rev.* **57**, 522 (1940).
15. P. Bucci, G. Ceccarelli and C. A. Veracini, *J. Chem. Phys.* **50**, 1510 (1969).
16. P. Bucci, M. Martinelli and S. Santucci, *J. Chem. Phys.* **52**, 4041 (1970).
17. P. Bucci, M. Martinelli and S. Santucci, *J. Chem. Phys.* **53**, 4524 (1970).
18. J. Biemond, J. A. B. Lohman and C. MacLean, *J. Magn. Reson.* **16**, 402 (1974).
19. H. Wennerström, N. O. Persson and B. Lindman, *J. Magn. Reson.* **13**, 348 (1974).
20. G. Lindblom, H. Wennerström and B. Lindman, *J. Magn. Reson.* **23**, 177 (1976).
21. R. B. Creel, E. D. von Meerwall and R. G. Barnes, *Chem. Phys. Lett.* **49**, 501 (1977).
22. R. E. McDonald and T. K. McNab, *Phys. Rev. Letters.* **32**, 1133 (1974).
23. D. Dubbers, K. Dörr, H. Ackermann, F. Fujara, H. Grupp, M. Grupp, P. Heitjans, A. Körblein and H. J. Stöckmann, *Z. Physik A*, **282**, 243 (1977).
24. V. J. Kowalewski, *Progress in NMR Spectroscopy*, **5**, p. 1, J. W. Emsley, J. Feeney and L. H. Sutcliffe (eds.), Pergamon Press, Oxford (1969).
25. R. Freeman and W. A. Anderson, *J. Chem. Phys.* **39**, 806 (1963).
26. E. B. Rawson and R. Beringer, *Phys. Rev.* **88**, 677 (1952).
27. V. W. Hughes and J. S. Geiger, *Phys. Rev.* **99**, 1842 (1955).
28. C. C. McDonald, *J. Chem. Phys.* **39**, 3159 (1963).
29. P. P. Sorokin, I. L. Gelles and W. V. Smith, *Phys. Rev.* **112**, 1513 (1958).
30. F. Chiarini, M. Martinelli and G. Ranieri, *J. Magn. Reson.* **14**, 60 (1974).
31. N. S. Dalal and A. Manoogian, *Phys. Rev. Lett.* **39**, 1573 (1977).
32. T. Oka and T. Shimizu, *Phys. Rev. A.* **2**, 587 (1970).
33. F. Chiarini, M. Martinelli, S. Santucci and P. Bucci, *Phys. Rev.* A **6**, 1300 (1972).
34. R. L. Williams, R. C. Haskell and L. Madansky, *Phys. Rev.* C **5**, 1435 (1972).
35. C. P. Slichter, *Principles of Magnetic Resonance*, Harper and Row, New York (1963).
36. R. L. Vold and R. R. Vold, *Progress in NMR Spectroscopy.* **12**, p. 79, J. W. Emsley, J. Feeney and L. H. Sutcliffe (eds.), Pergamon Press, Oxford (1978).
37. S. Schäublin, A. Höhener and R. R. Ernst, *J. Magn. Reson.* **13**, 196 (1974).
38. Antoine de Saint-Exupéry, *Le Petit Prince.*
39. P. L. Corio, *Structure of High Resolution NMR Spectra*, Academic Press, New York (1966).
40. G. Bodenhausen, R. L. Vold and R. R. Vold, *J. Magn. Reson.* **37**, 93 (1980).
41. G. L. Hoatson and K. J. Packer, *Mol. Phys.* **40**, 1153 (1980).
42. S. Vega and A. Pines, *J. Chem. Phys.* **66**, 5624 (1977).
43. H. Hatanaka, T. Ozawa and T. Hashi, *J. Phys. Soc. Japan*, **42**, 2069 (1977).
44. S. Vega and A. Pines, *Proc. XIX Congress Ampere, Heidelberg* 1976, K. H. Hausser and D. Schweizer (eds.), Beltz, Hemsback (1976).
45. A. Wokaun and R. R. Ernst, *Chem. Phys. Lett.* **52**, 407 (1977).
46. A. Pines, S. Vega, D. J. Ruben, T. W. Shattuck and D. E. Wemmer, *Proc. IV Ampere Int. Summer School*, Pula, Yugoslavia (1976).
47. W. P. Aue, E. Bartholdi and R. R. Ernst, *J. Chem. Phys.* **64**, 2229 (1976).
48. G. Drobny, A. Pines, S. Sinton, D. Weitekamp and D. Wemmer, *Faraday Div. Chem. Soc. Symp.* **13**, 49 (1979).
49. L. Müller, *J. Am. Chem. Soc.* **101**, 4481 (1979).
50. D. E. Wemmer, Ph.D. dissertation, Univ. Calif. Berkeley (1978).
51. H. Hatanaka, T. Terao and T. Hashi, *J. Phys. Soc. Japan*, **39**, 835 (1975).
52. E. K. Wolff, R. G. Griffin and C. Watson, *J. Chem. Phys.* **66**, 5433 (1977).
53. R. E. Stark, R. A. Haberkorn and R. G. Griffin, *J. Chem. Phys.* **68**, 1996 (1978).
54. E. Y. C. Lu and L. E. Wood, *Phys. Lett.* **44A**, 68 (1973).
55. R. G. Brewer and E. L. Hahn, *Phys. Rev. A* **11**, 1641 (1975).
56. S. Vega and Y. Naor, *J. Chem. Phys.* in press.
57. M. Polak and R. W. Vaughan, *Phys. Rev. Lett.* **39**, 1677 (1977).
58. M. Polak, A. J. Highe and R. W. Vaughan, *J. Magn. Reson.* **37**, 357 (1980).
59. M. E. Stoll, A. J. Vega and R. W. Vaughan, *Phys. Rev.* A **16**, 1521 (1977).
60. M. E. Stoll, A. J. Vega and R. W. Vaughan, *J. Chem. Phys.* **67**, 2029 (1977).
61. R. R. Ernst, *Fourth Int. Meeting on NMR Spectroscopy*, York, 1978.
62. G. Bodenhausen and D. J. Ruben, *Chem. Phys. Lett.* **69**, 185 (1980).
63. M. R. Roberts, D. A. Vidusek and G. Bodenhausen, *FEBS Lett.* **117**, 311 (1980).
64. A. Minoretti, W. P. Aue, M. Reinhold and R. R. Ernst, *J. Magn. Reson.* **40**, 175 (1980).
65. P. M. Henrichs and L. J. Schwartz, *J. Magn. Reson.* **28**, 477 (1977).

66. P. M. HENRICHS and L. J. SCHWARTZ, *J. Chem. Phys.* **69**, 622 (1978).
67. A. WOKAUN, Ph.D. Dissertation, ETH Zürich (1978).
68. H. HATANAKA and T. HASHI, *J. Phys. Soc. Japan*, **39**, 1139 (1975).
69. S. VEGA, *J. Chem. Phys.* **68**, 5518 (1978).
70. A. WOKAUN and R. R. ERNST, *J. Chem. Phys.* **67**, 1752 (1977).
71. R. POUPKO, R. L. VOLD and R. R. VOLD, *J. Magn. Reson.* **34**, 67 (1979).
72. R. L. VOLD, R. R. VOLD, R. POUPKO and G. BODENHAUSEN, *J. Magn. Reson.* **38**, 141 (1980).
73. S. R. HARTMANN and E. L. HAHN, *Phys. Rev.* **128**, 2042 (1962).
74. A. PINES, M. G. GIBBY and J. S. WAUGH, *J. Chem. Phys.* **59**, 569 (1973).
75. R. D. BERTRAND, W. B. MONIZ, A. N. GARROWAY and G. C. CHINGAS, *J. Am. Chem. Soc.* **100**, 5227 (1978).
76. R. D. BERTRAND, W. B. MONIZ, A. N. GARROWAY and G. C. CHINGAS, *J. Magn. Reson.* **32**, 465 (1978).
77. T. W. SHATTUCK, Ph.D. Dissertation, Univ. Calif. Berkeley (1976).
78. S. VEGA, T. W. SHATTUCK and A. PINES, *Phys. Rev.* **A22**, 638 (1980).
79. P. BRUNNER, M. REINHOLD and R. R. ERNST, *J. Chem. Phys.* **73**, 1086 (1980).
80. P. MANSFIELD and P. K. GRANNELL, *J. Phys. C* **4**, L197 (1971).
81. M. REINHOLD, P. BRUNNER and R. R. ERNST, *J. Chem. Phys.* **74** (1981).
82. W. S. WARREN, S. SINTON, D. P. WEITEKAMP and A. PINES, *Phys. Rev. Lett.* **43**, 1791 (1979); *J. Magn. Reson.* **40**, 581 (1980); *J. Chem. Phys.* **73**, 2084 (1980).
83. M. E. STOLL, E. K. WOLFF and M. MEHRING, *Phys. Rev. A* **17**, 1561 (1978).
84. E. K. WOLFF and M. MEHRING, *Phys. Lett.* **70A**, 125 (1979).
85. M. MEHRING, E. K. WOLFF and M. E. STOLL, *J. Magn. Reson.* **37**, 475 (1980).
86. I. SOLOMON, *Phys. Rev.* **110**, 61 (1958).
87. R. R. ERNST, *Adv. Magn. Reson.* **2**, p. 1. J. S. WAUGH (ed.), Academic Press, New York (1966).
88. W. P. AUE, P. BACHMANN, A. WOKAUN and R. R. ERNST, *J. Magn. Reson.* **29**, 523 (1978).
89. J. JEENER, *Ampere International Summer School, Basko Polje*, Yugoslavia (1971).
90. R. N. BRACEWELL, *The Fourier Transform and its Applications*, McGraw-Hill, New York (1978).
91. A. WOKAUN and R. R. ERNST, *Mol. Phys.* **36**, 317 (1978).
92. S. HSI, H. ZIMMERMANN and Z. LUZ, *J. Chem. Phys.* **69**, 4126 (1978).
93. A. A. MAUDSLEY and R. R. ERNST, *Chem. Phys. Lett.* **50**, 368 (1977).
94. A. PINES, D. WEMMER, J. TANG and S. SINTON, *Bull. Am. Phys. Soc.* **23**, 21 (1978).
95. A. BAX, P. G. DE JONG, A. F. MEHLKOPF and J. SMIDT, *Chem. Phys. Lett.* **69**, 567 (1980).
96. S. VEGA, T. W. SHATTUCK and A. PINES, *Phys. Rev. Lett.* **37**, 43 (1976).
97. A. ABRAGAM, *The Principles of Nuclear Magnetism*, Oxford University Press (1961).
98. A. D. BUCKINGHAM and K. A. MCLAUCHLAN, *Progress in NMR Spectroscopy*, **2**, p. 63, J. W. EMSLEY, J. FEENEY and L. H. SUTCLIFFE (eds.), Pergamon Press, Oxford (1967).
99. P. DIEHL and C. L. KHETRAPAL, *NMR Basic Principles and Progress*, **1**, p. 1, P. DIEHL, E. FLUCK and R. KOSFELD (eds.), Springer (1969).
100. J. W. EMSLEY and J. C. LINDON, *NMR Spectroscopy Using Liquid Crystal Solvents*, Pergamon Press, Oxford (1975).
101. A. SAUPE, *Z. Naturforsch.* **20A**, 572 (1965).
102. R. A. HOFFMAN and S. FORSÉN, *Progress in NMR Spectroscopy*, **1**, p. 15, J. W. EMSLEY, J. FEENEY and L. H. SUTCLIFFE (eds.), Pergamon Press, Oxford (1966).
103. R. FREEMAN and D. H. WHIFFEN, *Mol. Phys.* **4**, 321 (1961).
104. W. A. ANDERSON and R. FREEMAN, *J. Chem. Phys.* **37**, 85 (1962).
105. R. FREEMAN and W. A. ANDERSON, *J. Chem. Phys.* **37**, 2053 (1962).
106. A. WOKAUN and R. R. ERNST, *Mol. Phys.* **38**, 1579 (1979).
107. A. L. BLOOM and J. N. SHOOLERY, *Phys. Rev.* **97**, 1261 (1955).
108. J. W. EMSLEY, J. C. LINDON and J. M. TABONY, *J. Chem. Soc. Faraday Trans.* 2, **69**, 10 (1973).
109. L. C. SNYDER and S. MEIBOOM, *J. Chem. Phys.* **58**, 5096 (1973).
110. R. C. HEWITT, S. MEIBOOM and L. C. SNYDER, *J. Chem. Phys.* **58**, 5089 (1973).
111. A. PINES, D. J. RUBEN, S. VEGA and M. MEHRING, *Phys. Rev. Lett.* **36**, 110 (1976).
112. A. PINES, S. VEGA and M. MEHRING, *Phys. Rev. B*, **18**, 112 (1978).
113. D. SUWELACK, M. MEHRING and A. PINES, *Phys. Rev. B*, **19**, 238 (1979).
114. W. P. AUE, J. KARHAN and R. R. ERNST, *J. Chem. Phys.* **64**, 4226 (1976).
115. G. BODENHAUSEN and C. M. DOBSON, to be published.
116. G. BODENHAUSEN, N. M. SZEVERENYI, R. L. VOLD and R. R. VOLD, *J. Am. Chem. Soc.* **100**, 6265 (1978).
117. E. L. HAHN, *Phys. Rev.* **80**, 580 (1950).
118. E. L. HAHN and D. E. MAXWELL, *Phys. Rev.* **88**, 1070 (1952).
119. H. Y. CARR and E. M. PURCELL, *Phys. Rev.* **94**, 630 (1954).
120. S. MEIBOOM and D. GILL, *Rev. Sci. Instrum.* **29**, 688 (1958).
121. G. BODENHAUSEN and R. FREEMAN, *J. Magn. Reson.* **28**, 303 (1977).
122. R. L. VOLD and S. O. CHAN, *J. Chem. Phys.* **53**, 449 (1970).
123. R. FREEMAN and H. D. W. HILL, *J. Chem. Phys.* **54**, 301 (1971).
124. A. A. MAUDSLEY, A. WOKAUN and R. R. ERNST, *Chem. Phys. Lett.* **55**, 9 (1978).
125. H. C. TORREY, *Phys. Rev.* **76**, 1059 (1949).
126. I. SOLOMON, *Phys. Rev. Lett.* **2**, 301 (1959).
127. I. SOLOMON, *Compt. rend.* **248**, 92 (1959).
128. I. SOLOMON, *Compt. rend.* **249**, 1631 (1959).
129. H. HATANAKA and T. HASHI, *Phys. Lett.* **67A**, 183 (1978).
130. A. G. REDFIELD, *Phys. Rev.* **101**, 67 (1956).
131. H. HATANAKA and T. HASHI, *Phys. Rev. B*, **21**, 2677 (1980).
132. T. HASHI, to be published.
133. A. G. REDFIELD, *Adv. Magn. Reson.* **1**, p. 1, J. S. WAUGH (ed.), Academic Press, New York (1965).
134. R. R. VOLD and R. L. VOLD, *J. Chem. Phys.* **66**, 4018 (1977).
135. N. M. SZEVERENYI, Ph.D. Dissertation, Univ. Calif., San Diego (1978).
136. R. FREEMAN, S. WITTEKOEK and R. R. ERNST, *J. Chem. Phys.* **52**, 1529 (1970).
137. J. TANG and A. PINES, *J. Chem. Phys.* **72**, 3290 (1980).
138. R. L. VOLD, J. S. WAUGH, M. P. KLEIN and D. E. PHELPS, *J. Chem. Phys.* **48**, 3831 (1968).
139. D. E. DEMCO, P. VAN HECKE and J. S. WAUGH, *J. Magn. Reson.* **16**, 467 (1974).
140. R. R. VOLD and G. BODENHAUSEN, *J. Magn. Reson.* **39**, 363 (1980).
141. J. JEENER and P. BROEKAERT, *Phys. Rev.* **157**, 9 (1967).
142. S. EMID, A. BAX, J. KONIJNENDIJK, J. SMIDT and A. PINES, *Physica*, **96B**, 333 (1979).

143. L. MÜLLER and R. R. ERNST, *Mol. Phys.* **38**, 963 (1979).
144. K. NAGAYAMA, *J. Chem. Phys.* **71**, 4404 (1979).
145. G. BODENHAUSEN, *J. Magn. Reson.* **34**, 357 (1979).
146. A. BAX, R. FREEMAN and S. P. KEMPSELL, *J. Am. Chem. Soc.* **102**, 4849 (1980); *J. Magn. Reson.* **41**, 349 (1980).
147. R. ECKMAN, L. MÜLLER and A. PINES, *Chem. Phys. Lett.* **74**, 376 (1980).